

第二届超边缘碰撞物理研讨会

Strong Electromagnetic Fields, UPC and EIC/Eicc



Perturbative calculation of spin polarization in central, peripheral and ultraperipheral heavy-ion collisions

Shanshan Cao

Shandong University

April 14, 2024 @ USTC

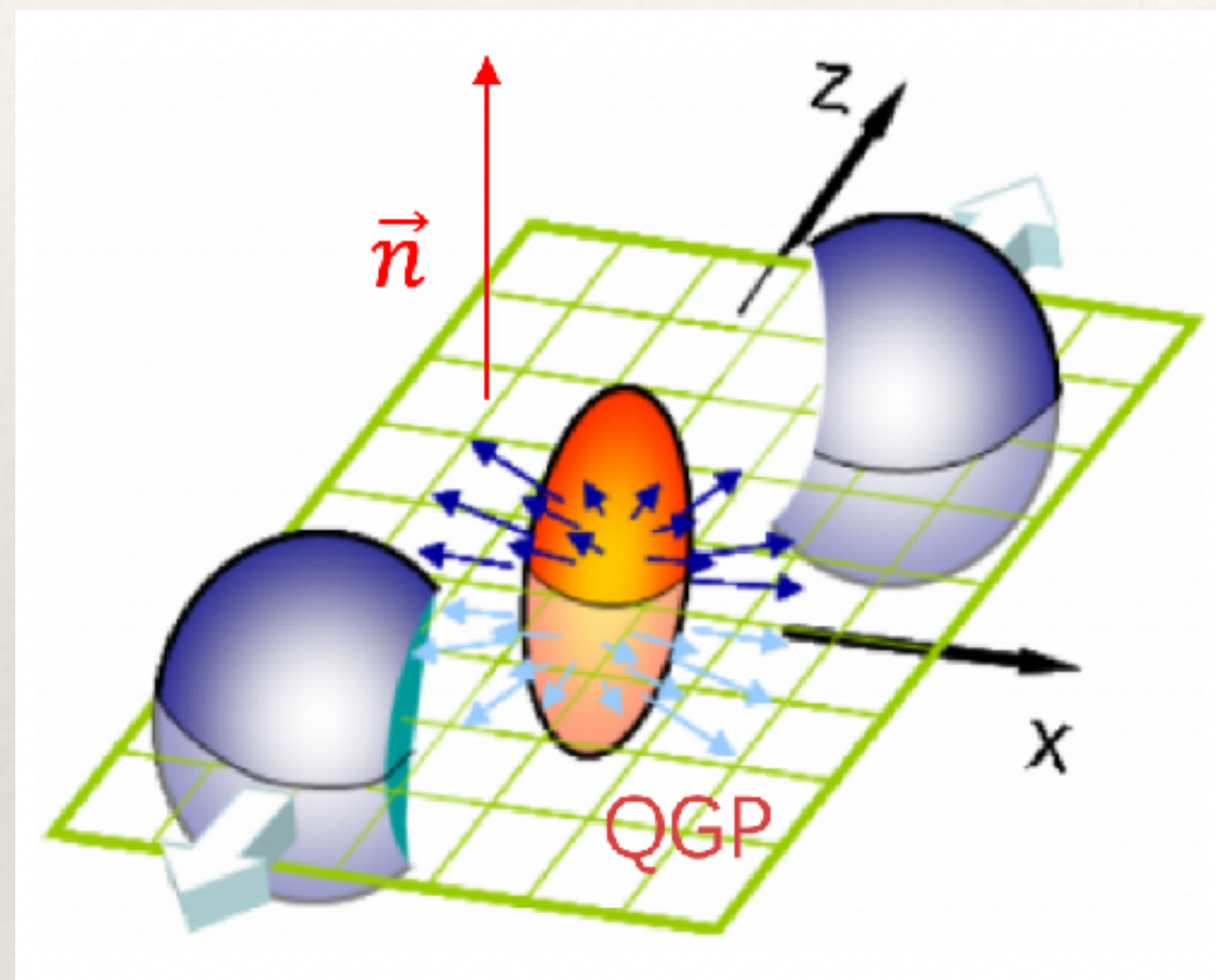


Outline

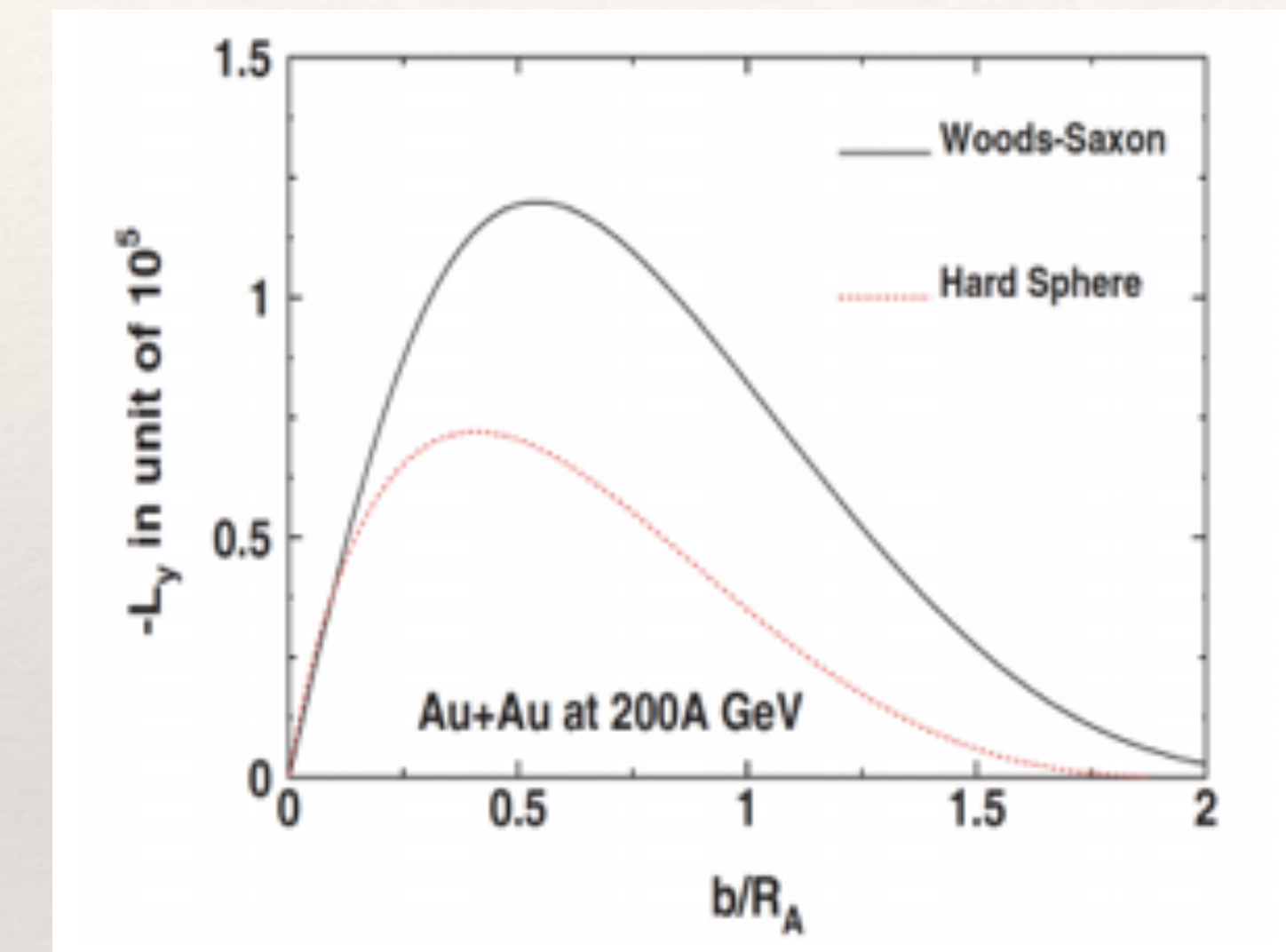
- **Introduction**
- **Production and evolution of the QGP global polarization**
[X. Li, Z.-F. Jiang, SC, J. Deng, Eur. Phys. J. C 83 (2023) 1, 96]
- **Spin polarization from jet fragmentation**
[X. Li, Z.-X. Chen, SC, S.-Y. Wei, Phys. Rev. D 109 (2024) 1, 014035]
- **Summary**

Spin-orbital coupling in a strongly interacting system

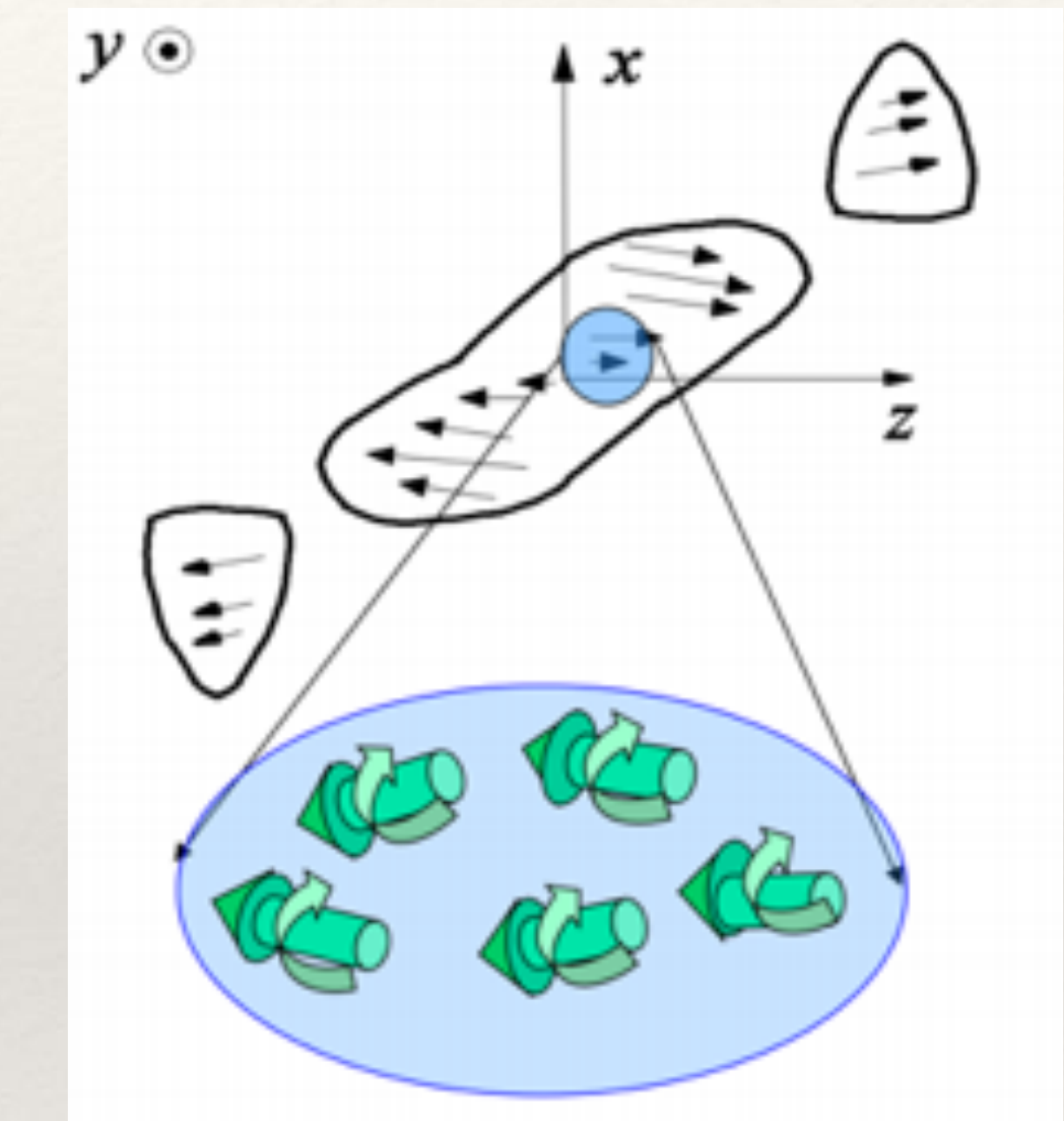
Non-central relativistic
heavy-ion collisions



Huge orbital angular
momentum



Global polarization



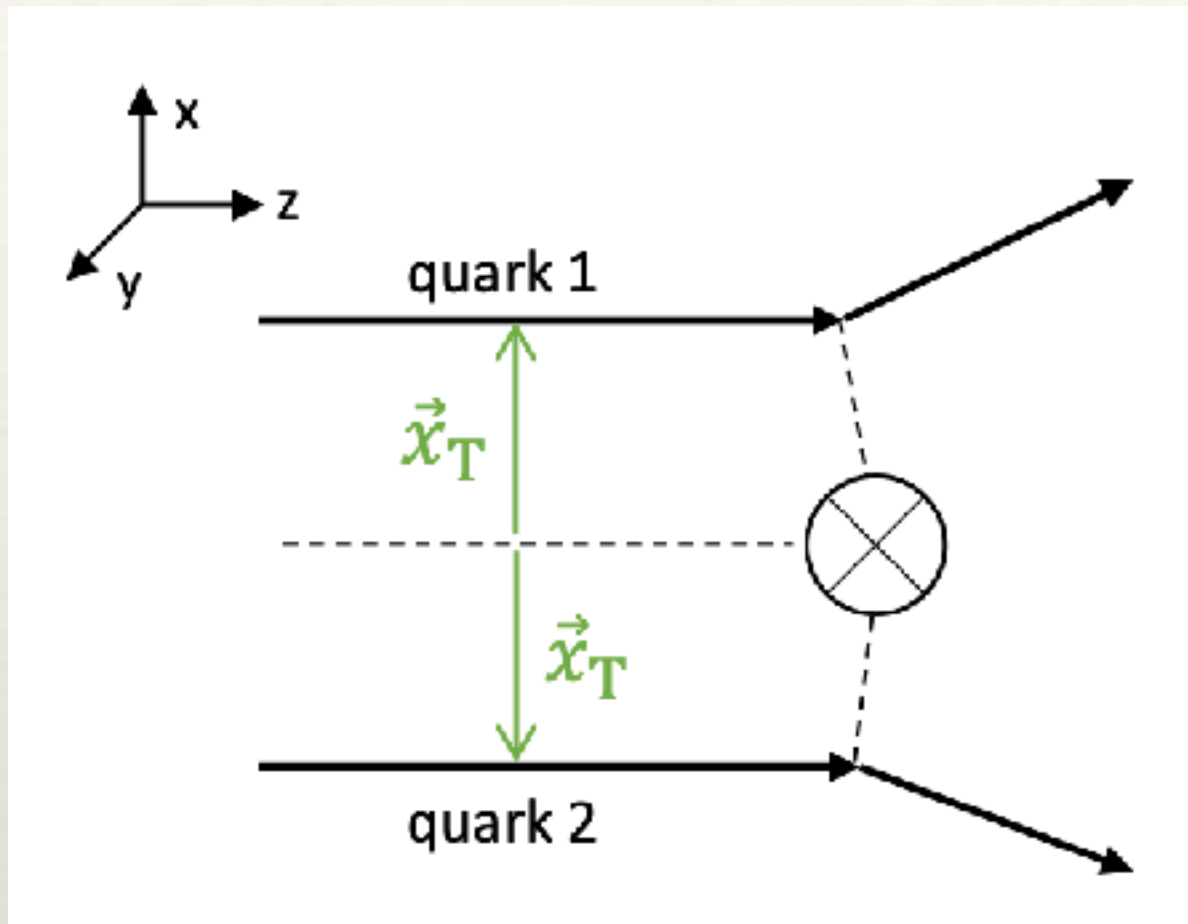
$$\hat{n} = \frac{\vec{b} \times \vec{P}}{|\vec{b} \times \vec{P}|} = -\hat{y}$$

J.-H. Gao, S.-W. Chen, W.-T. Deng, Z.-T. Liang, Q. Wang, X.-N. Wang, Phys. Rev. C 77 (2008) 044902

Z.-T. Liang and X.-N. Wang, Phys. Rev. Lett. 94 (2005) 102301

A brief review of the first calculation of global polarization

Quark-potential scattering model [Z.-T. Liang and X.-N. Wang, Phys. Rev. Lett. 94 (2005) 102301]



Consider a quark (quark 1) scattering with a potential

$$A_0(q_T) = g/(q_T^2 + \mu^2)$$

Initial momentum (E, \vec{p}) , final spin $\lambda/2$ along \hat{n} ($-\hat{y}$)

Differential cross section w.r.t. \vec{x}_T :

$$\frac{d^2\sigma_\lambda}{d^2x_T} = C_T \int \frac{d^2q_T}{(2\pi)^2} \frac{d^2k_T}{(2\pi)^2} e^{i(\vec{k}_T - \vec{q}_T) \cdot \vec{x}_T} \mathcal{I}_\lambda$$

(Fourier transform into the coordinate space)

$$\mathcal{I}_\lambda = \frac{g^2}{2(2E)^2} \bar{u}_\lambda(p_q) \not{A}(q_T)(\not{p} + m) \not{A}(k_T) u_\lambda(p_k)$$

(Final spin not summed)

A brief review of the first calculation of global polarization

With small angle approximation

Spin-independent cross section:

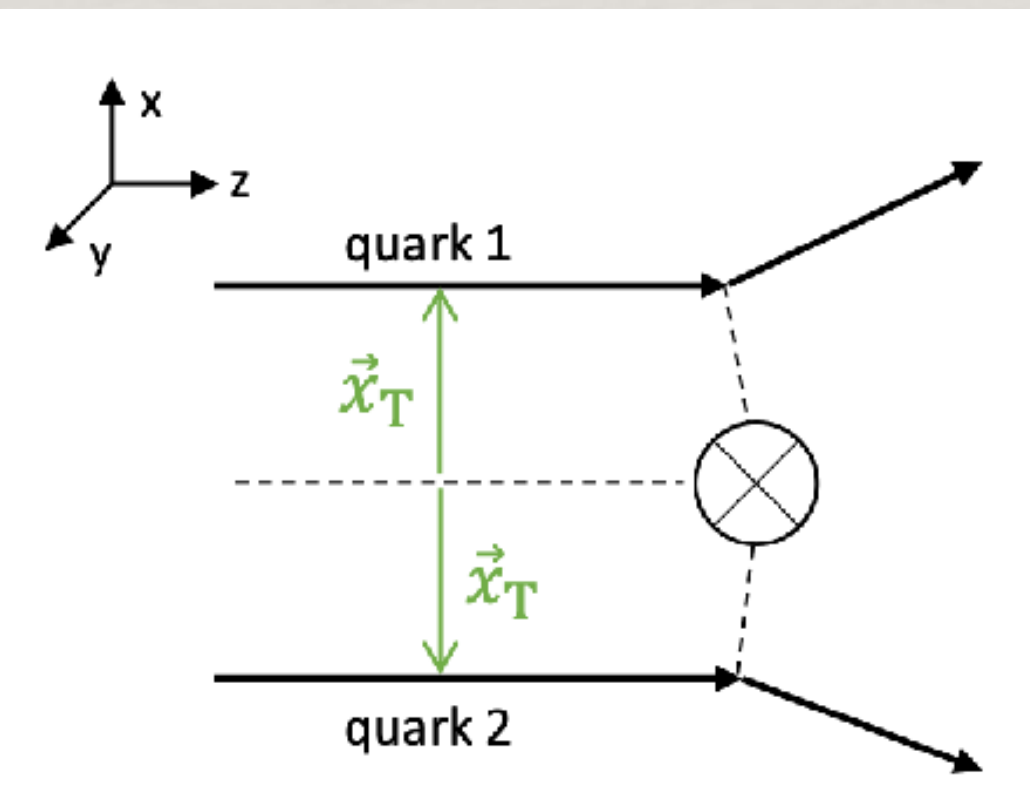
$$\frac{d\sigma}{d^2x_T} = \frac{d\sigma_+}{d^2x_T} + \frac{d\sigma_-}{d^2x_T} = 4C_T\alpha_s^2 K_0^2(\mu x_T)$$

Spin-dependent cross section:

$$\frac{d\Delta\sigma}{d^2x_T} = \frac{d\sigma_+}{d^2x_T} - \frac{d\sigma_-}{d^2x_T} = -4C_T\alpha_s^2 \mu \frac{\vec{p} \cdot (\hat{x}_T \times \hat{n})}{E(E+m)} K_0(\mu x_T) K_1(\mu x_T)$$

Polarization:

$$P = \frac{\Delta\sigma}{\sigma} = \frac{\sigma_+ - \sigma_-}{\sigma_+ + \sigma_-} = \frac{\int_0^\infty dx \int_{-\infty}^\infty dy \frac{d\Delta\sigma}{dxdy}}{\int_0^\infty dx \int_{-\infty}^\infty dy \frac{d\sigma}{dxdy}} = -\frac{\pi\mu p}{2E(E+m)}$$

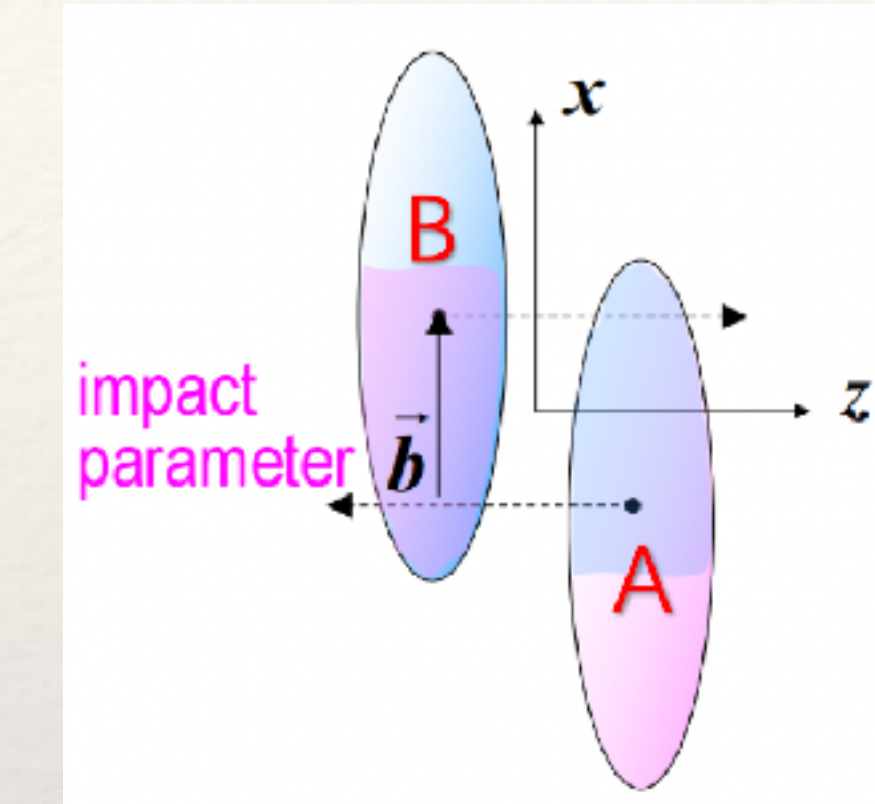
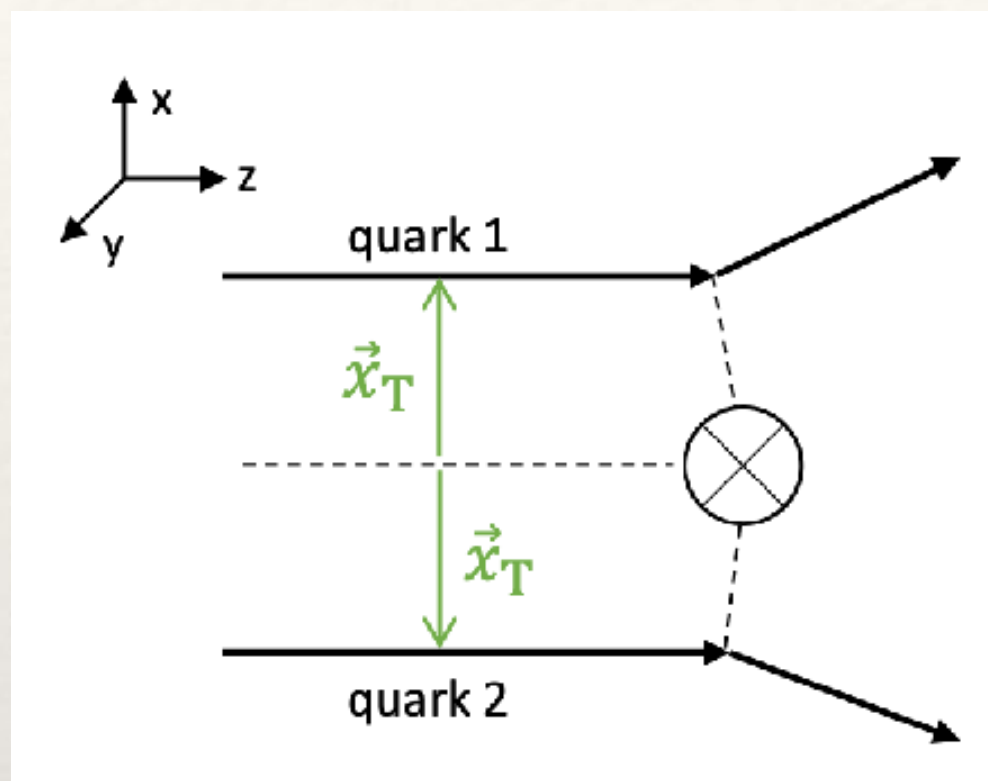


Caveats:

- Integration over only half plane (0 if over the whole plane)
- Approximating the whole nuclear matter with a single potential
- Only single scattering, no evolution

Model improvement

For a single quark from nucleus A scattering with the whole nucleus B



$T(x,y)$: participant number distribution in nucleus B (Glauber)

$$P = \frac{\Delta\sigma}{\sigma} = \frac{\sigma_+ - \sigma_-}{\sigma_+ + \sigma_-} = \frac{\int_0^\infty dx \int_{-\infty}^\infty dy \frac{d\Delta\sigma}{dxdy}}{\int_0^\infty dx \int_{-\infty}^\infty dy \frac{d\sigma}{dxdy}}$$

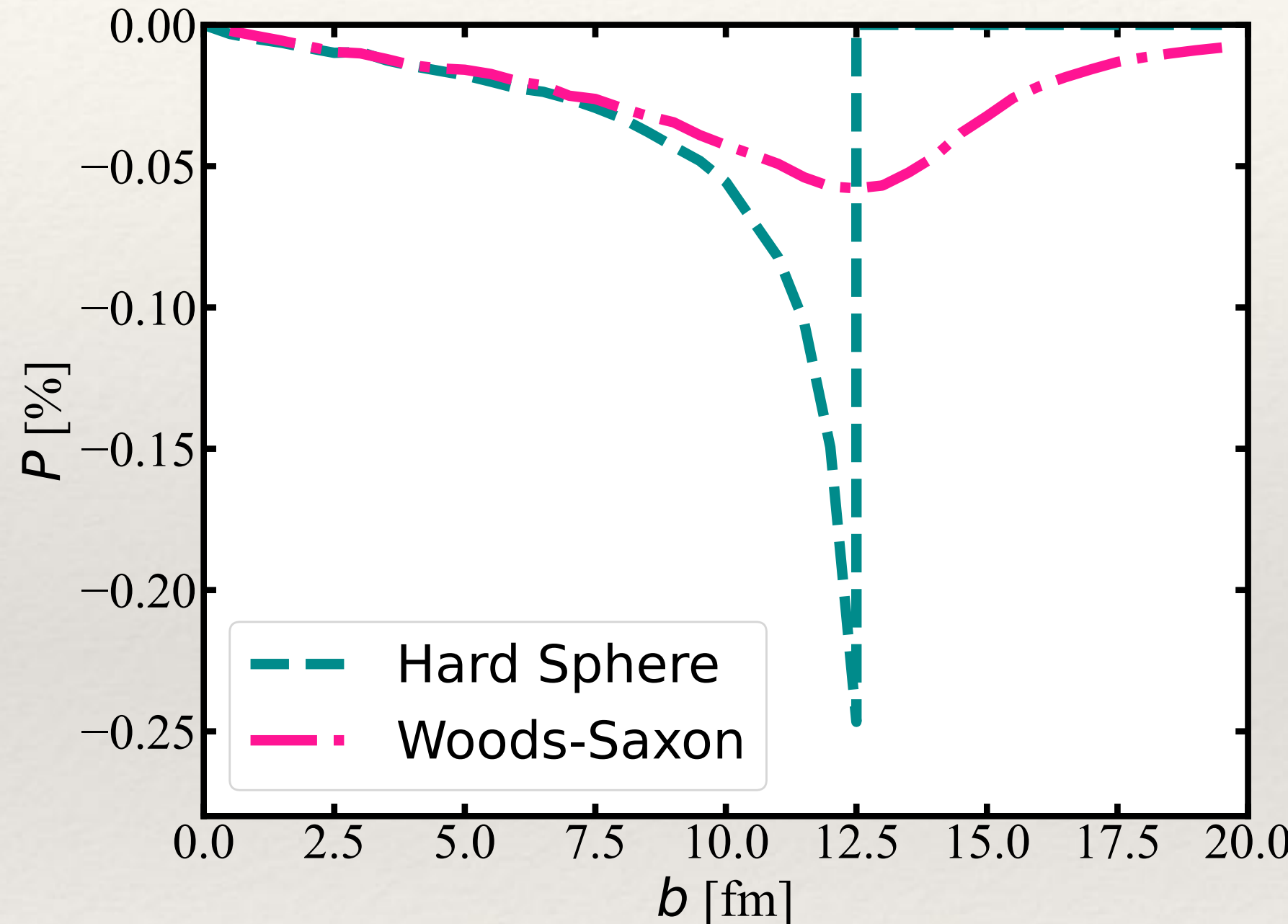
$$P = \frac{\int T(x,y) \frac{d\Delta\sigma(x,y)}{d^2x_T} d^2x_T}{\int T(x,y) \frac{d\sigma(x,y)}{d^2x_T} d^2x_T}$$

Interact with one scattering center in a half plane

Interact with multiple scattering centers distributed according to nuclear density

Transverse plane averaged polarization from initial collisions

$$\overline{P} = \frac{\int [T_1(x,y)\Delta\mathcal{P}_A(x,y) + T_2(x,y)\Delta\mathcal{P}_B(x,y)]dxdy}{\int [T_1(x,y)\mathcal{P}_A(x,y) + T_2(x,y)\mathcal{P}_B(x,y)]dxdy}$$



- Overall negative value of polarization (along $-\hat{y}$ direction)
- Noticeable difference between HS and WS calculations only at large impact parameter

Multiple scatterings inside the QGP

For polarized initial quark state [X.-G. Huang, P. Huovinen, X.-N. Wang, Phys. Rev. C 84 (2011) 054910]

$$\frac{d\sigma_\lambda}{dx_T^2} = \frac{1}{2} g^4 C_T \left[\frac{1}{4\pi^2} (1 + \lambda_f \textcolor{red}{P}_i) K_0^2(\mu x_T) - \frac{\mu}{4\pi^2} K_0(\mu x_T) K_1(\mu x_T) \frac{1}{E(E+m)} (\lambda_f + \textcolor{red}{P}_i) \vec{p} \cdot (\vec{n} \times \vec{x}_T) \right]$$

Spin-independent cross section:

$$\frac{d\sigma}{d^2x_T} = \frac{d\sigma_+}{d^2x_T} + \frac{d\sigma_-}{d^2x_T}$$

Spin-dependent cross section:

$$\frac{d\Delta\sigma}{d^2x_T} = \frac{d\sigma_+}{d^2x_T} - \frac{d\sigma_-}{d^2x_T}$$

Polarization of final quark state:

$$P_f(x, y) = \frac{\int dx_1 dy_1 \textcolor{red}{s}(x_1, y_1) \frac{d\Delta\sigma(x, y, x_1, y_1)}{dx_1 dy_1}}{\int dx_1 dy_1 \textcolor{red}{s}(x_1, y_1) \frac{d\sigma(x, y, x_1, y_1)}{dx_1 dy_1}}$$

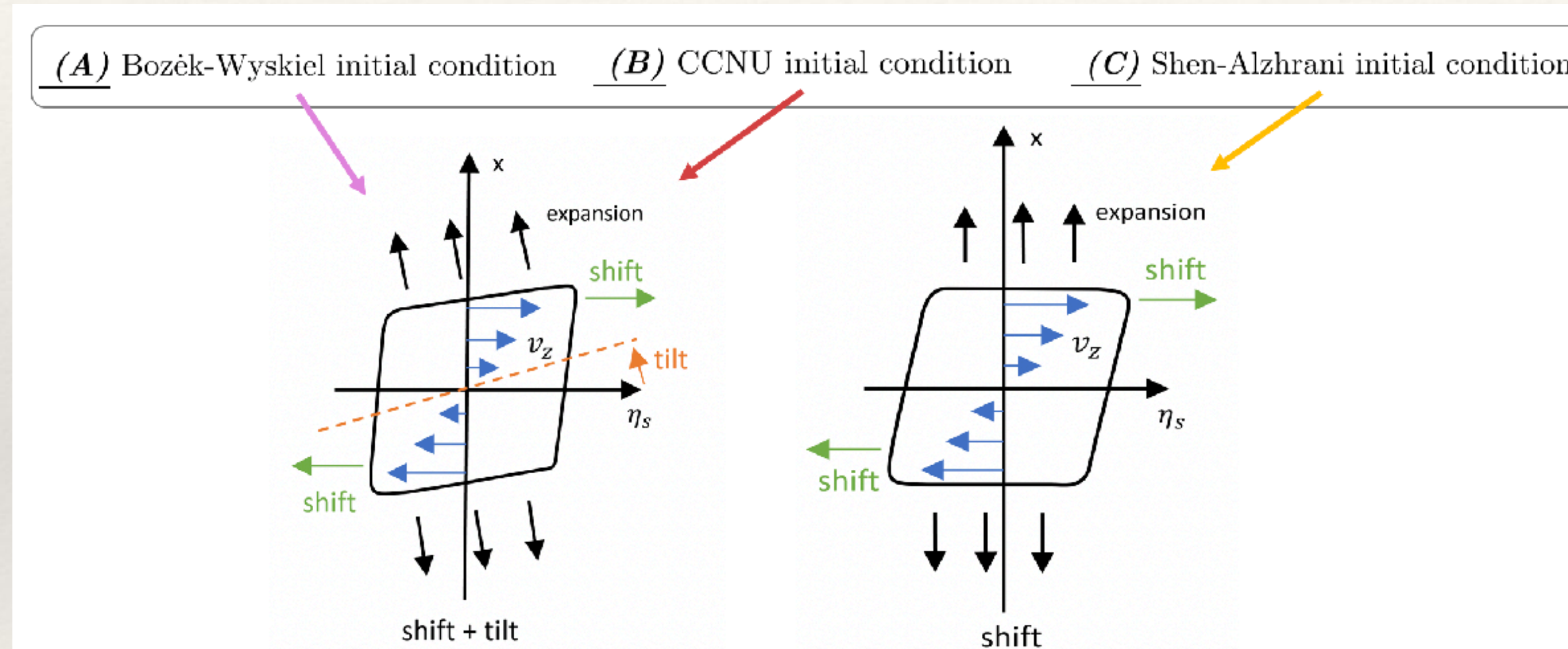
(s : entropy density of the QGP, from hydrodynamic model)

Time evolution of polarization:

$$\frac{dP(x, y)}{dt} = \frac{\Delta P(x, y)}{\tau_q} = \frac{4T\rho}{9s} \frac{s}{\eta_v} \Delta P(x, y) \quad (\Delta P = P_f - P_i)$$

Application of hydrodynamic model

- (3+1)-D CLVisc hydrodynamic model [L.-G. Pang, H. Petersen, X.-N. Wang, Phys. Rev. C 97 (2018) 064918; X.-Y. Wu, L.-G. Pang, G.-Y. Qin, X.-N. Wang, Phys. Rev. C 98 (2018) 024913]
- Compare three different initial geometries



- (A) P. Bozek and I. Wyskiel, Phys. Rev. C 81 (2010) 054902
 (B) Z.-F. Jiang, C.-B. Yang, Q. Peng, Phys. Rev. C 104 (2021) 064903
 (C) S. Ryu, V. Jupic, C. Shen, Phys. Rev. C 104 (2021) 054908

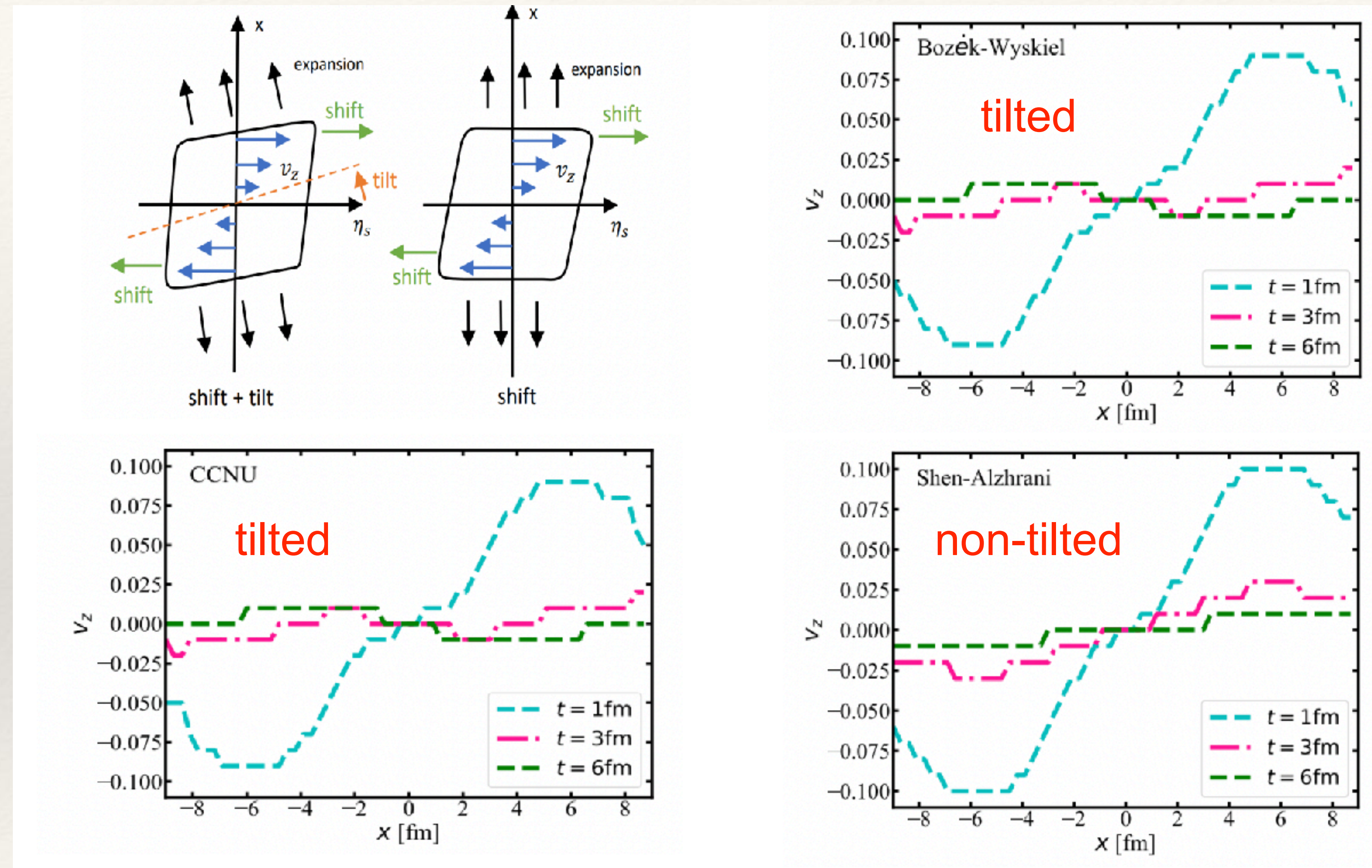
- Introduce initial longitudinal flow $v_{\eta_s} = T^{\tau\eta}/T^{\tau\tau}$

$$T^{\tau\tau}(x, y, \eta_s) = \epsilon(x, y, \eta_s) \cosh(y_L)$$

$$T^{\tau\eta}(x, y, \eta_s) = \frac{1}{\tau_0} \epsilon(x, y, \eta_s) \sinh(y_L)$$

[S. Ryu, V. Jupic, C. Shen, Phys. Rev. C 104 (2021) 054908]

Evolution of longitudinal velocity at $z = 0$ plane



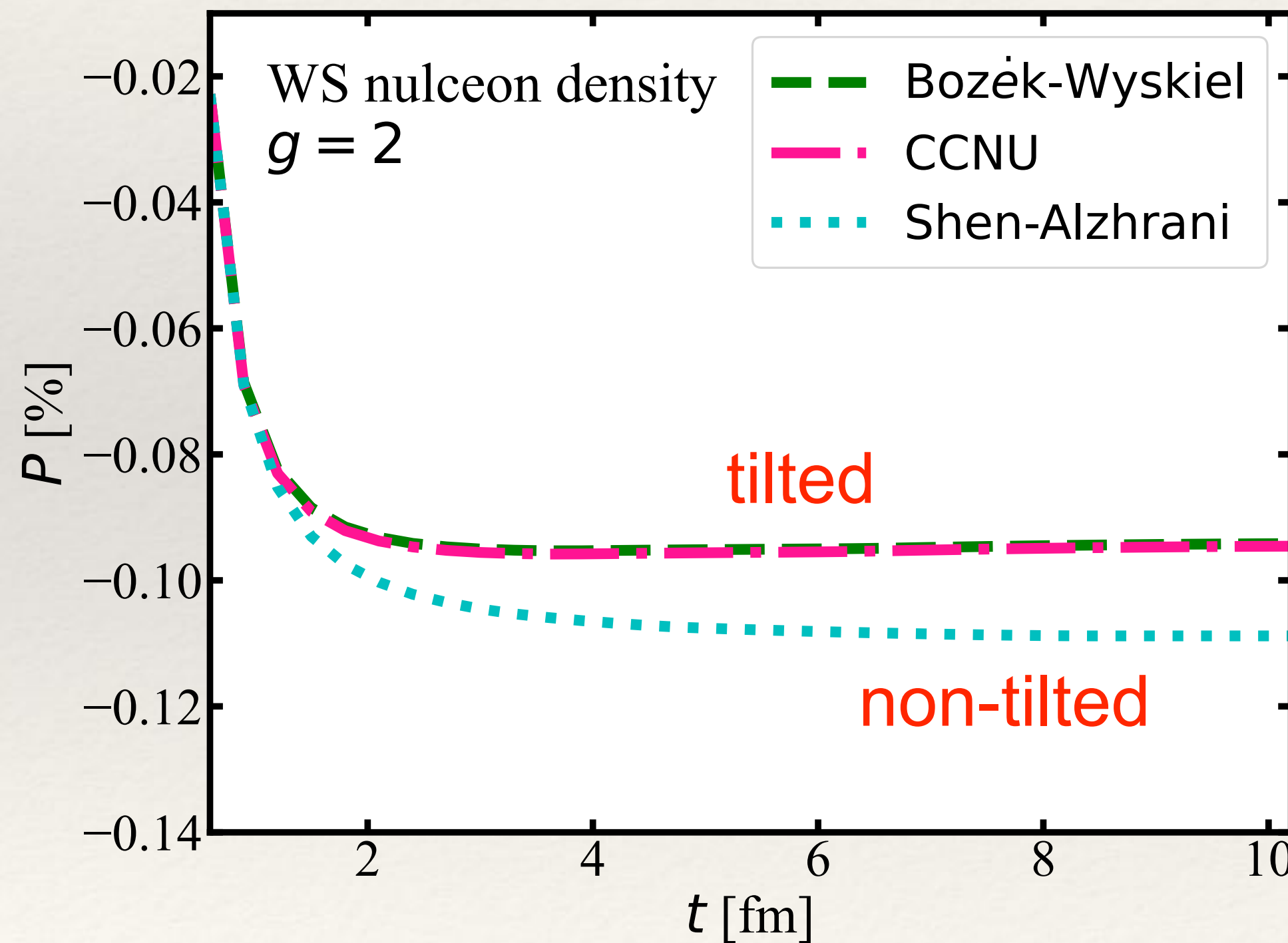
Sensitive to the initial geometry: tilted geometry reduces the longitudinal flow faster, even flip its sign

Time evolution of the average global polarization

Increment of global polarization during one time step:

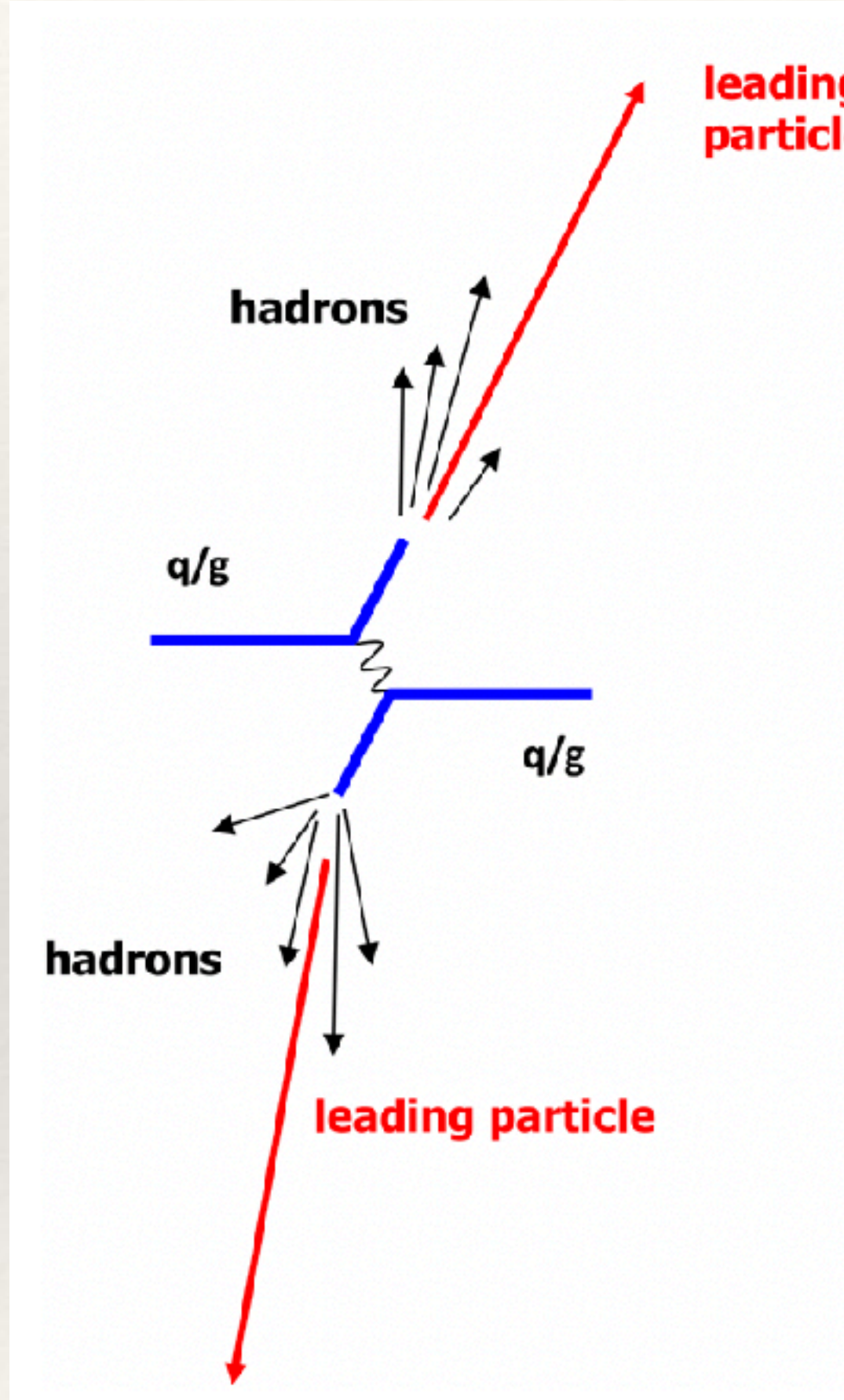
$$\overline{\Delta P}(t) = \frac{\int_{T > T_{\text{frz}}} dx dy s(x,y,t) \Delta P(x,y,t)}{\int dx dy s(x,y,t)}$$

Update of polarization: $\overline{P}(t + \Delta t) = \overline{P}(t) + \overline{\Delta P}(t)$



- Increase (in magnitude) of polarization from an initial value given by initial hard scatterings
- Evolution of polarization in QGP depends on the QGP initial condition
- About 15% difference in the final global polarization due to different initial condition

Another source of hadron polarization — jet fragmentation



- In pp collisions:

$$d\sigma_h = \sum_{abjd} f_{a/p} \otimes f_{b/p} \otimes d\sigma_{ab \rightarrow jd} \otimes D_{h/j}$$

- In AA collisions (QGP modification of jet parton):

$$d\tilde{\sigma}_h = \sum_{abjdj'} f_{a/A} \otimes f_{b/B} \otimes d\sigma_{ab \rightarrow jd} \otimes P_{j \rightarrow j'} \otimes D_{h/j'}$$

- Fragmentation function (FF):

$$D_{q \rightarrow h}(z, S, S_q) = D_1(z) + \lambda_q \lambda_h G_{1L}(z) + \vec{S}_{q\perp} \cdot \vec{S}_T H_{1T}(z)$$

unpolarized, polarized (longitudinal and transverse)

Constraints on longitudinal spin transfer

- Good constraints on unpolarized FFs, early stage for polarized FFs
- Example: DSV FFs to Λ hyperons [de Florian, Stratmann, Vogelsang, Phys. Rev. D 57 (1998) 5811]

Unpolarized parts: $D_1^{u \rightarrow \Lambda} = D_1^{d \rightarrow \Lambda} = D_1^{s \rightarrow \Lambda}$

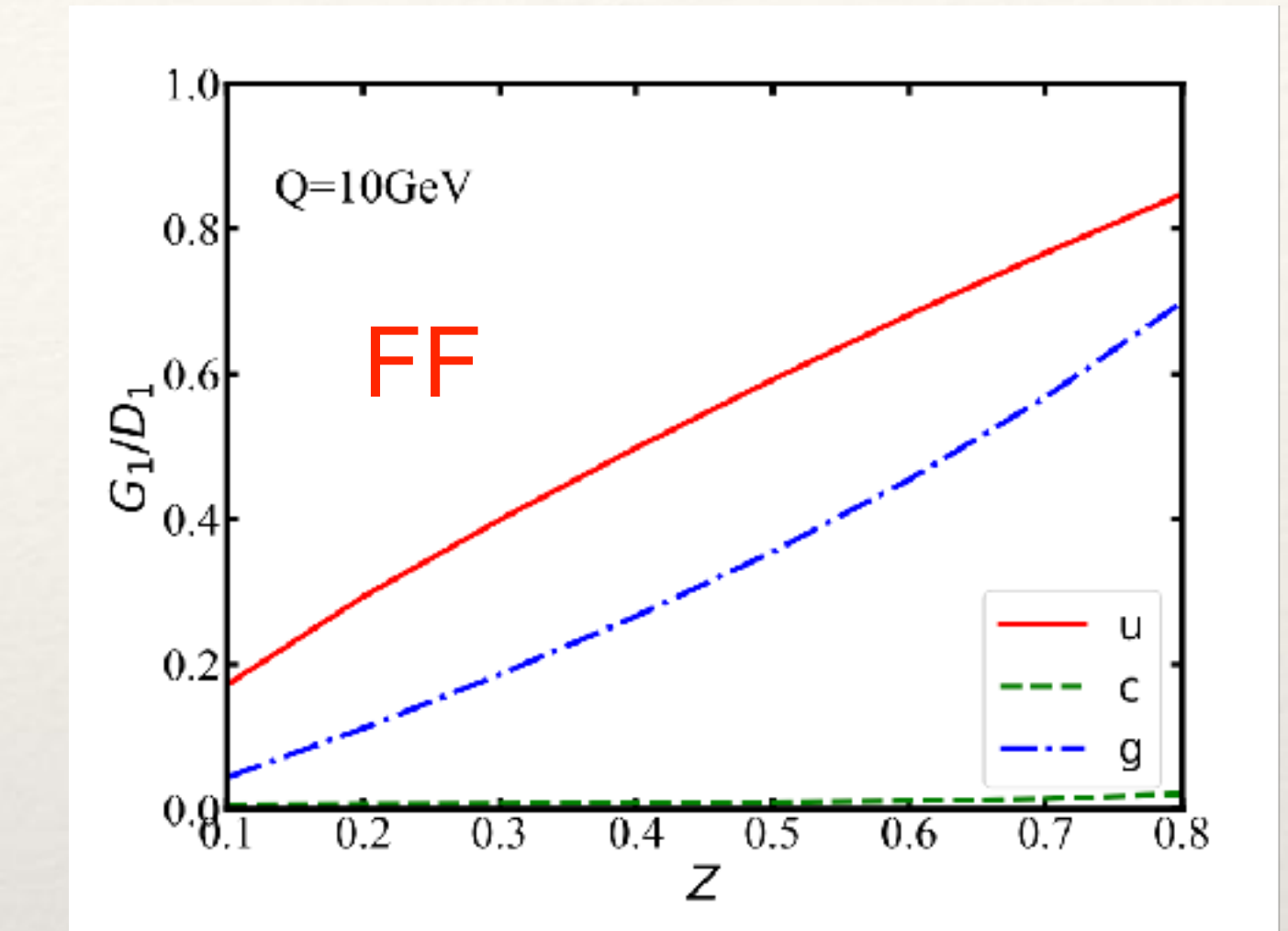
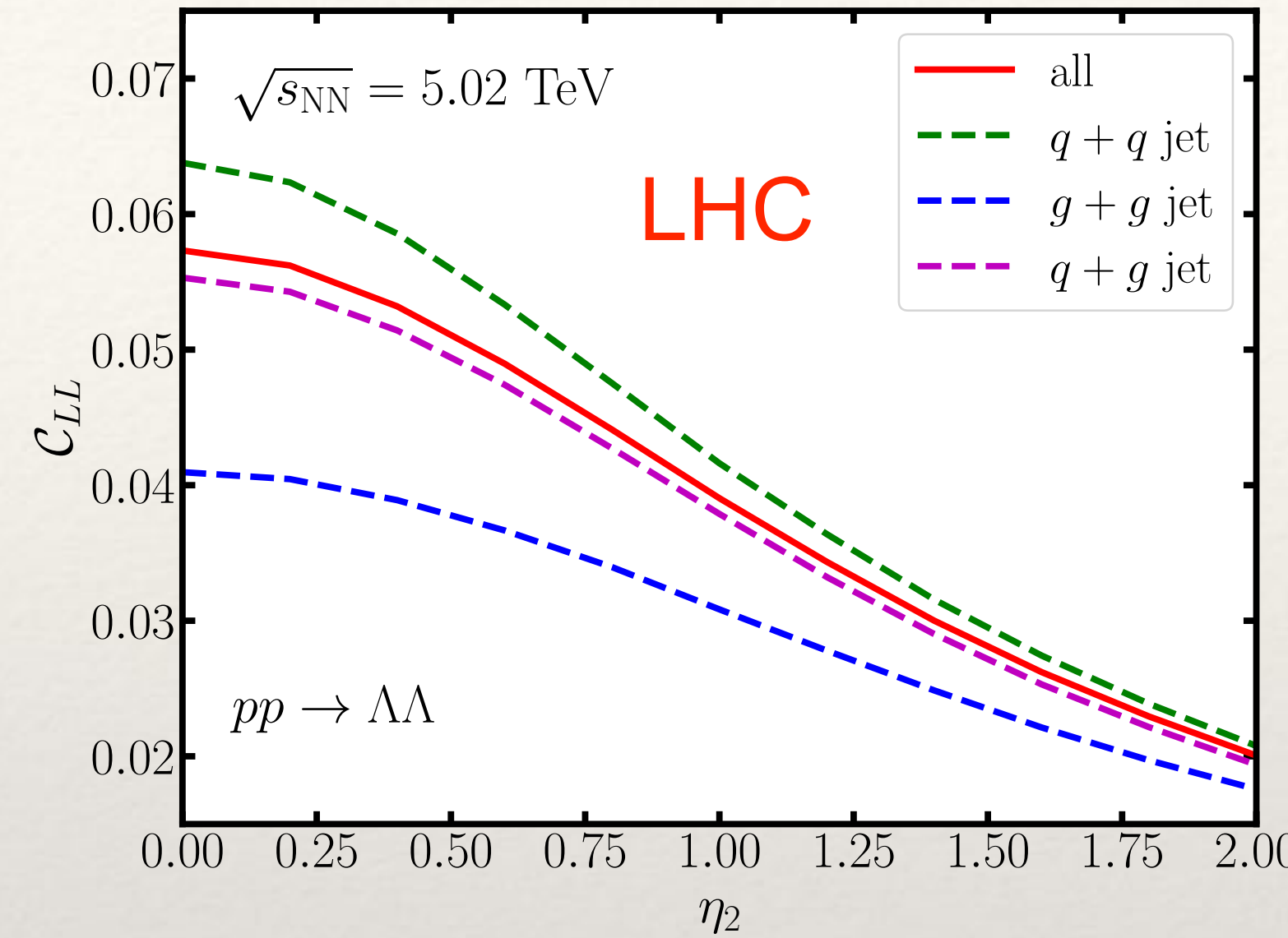
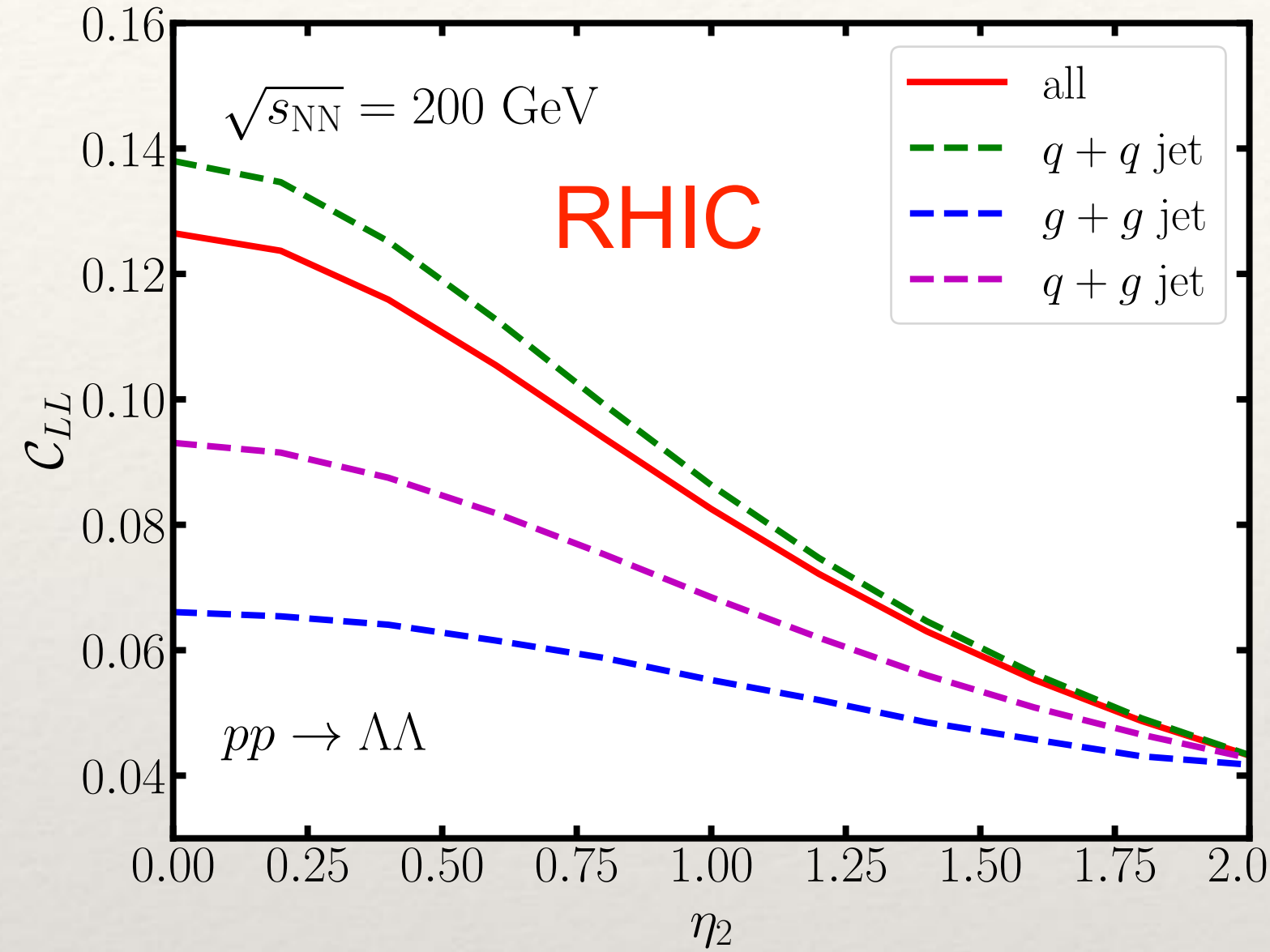
Polarized parts: $G_{1L}^{u \rightarrow \Lambda} = G_{1L}^{d \rightarrow \Lambda} = \xi G_{1L}^{s \rightarrow \Lambda}$ ($G_{1L}^{g \rightarrow \Lambda} = G_{1L}^{c \rightarrow \Lambda} = 0$ at initial scale)

Scenario 1: $\xi = 0$; Scenario 2: $\xi = -0.2$; Scenario 3: $\xi = 1$

- Usual measurements of G_{1L} with polarized beams or weak-interaction-dominating reactions
- Proposal on constraining G_{1L} using the correlation of dihadron polarization (neither polarized beam nor weak interaction process) [H.-C. Zhang and S.-Y. Wei, Phys. Lett. B 839 (2023) 137821]

$$\mathcal{C}_{LL}(\eta_1, \eta_2) = \left(\frac{d\sigma_{\lambda_1=\lambda_2}}{d\eta_1 d\eta_2} - \frac{d\sigma_{\lambda_1=-\lambda_2}}{d\eta_1 d\eta_2} \right) \Bigg/ \left(\frac{d\sigma_{\lambda_1=\lambda_2}}{d\eta_1 d\eta_2} + \frac{d\sigma_{\lambda_1=-\lambda_2}}{d\eta_1 d\eta_2} \right)$$

Correlation of dihadron polarization in pp collisions



- $\Lambda\Lambda$ production: t -channel dominating, prefers same sign of partonic λ_1 and λ_2
- $\mathcal{C}_{LL}^{q+q} > \mathcal{C}_{LL}^{q+g} > \mathcal{C}_{LL}^{g+g}$: smaller longitudinal spin transfer from g than from q to Λ
- $\mathcal{C}_{LL}(\text{RHIC}) > \mathcal{C}_{LL}(\text{LHC})$: larger z probed at RHIC and larger q contribution at RHIC

From pp to AA collisions

- Motivation: increase luminosity for experimental measurement
- Dihadron cross section in AA collisions at the leading order:

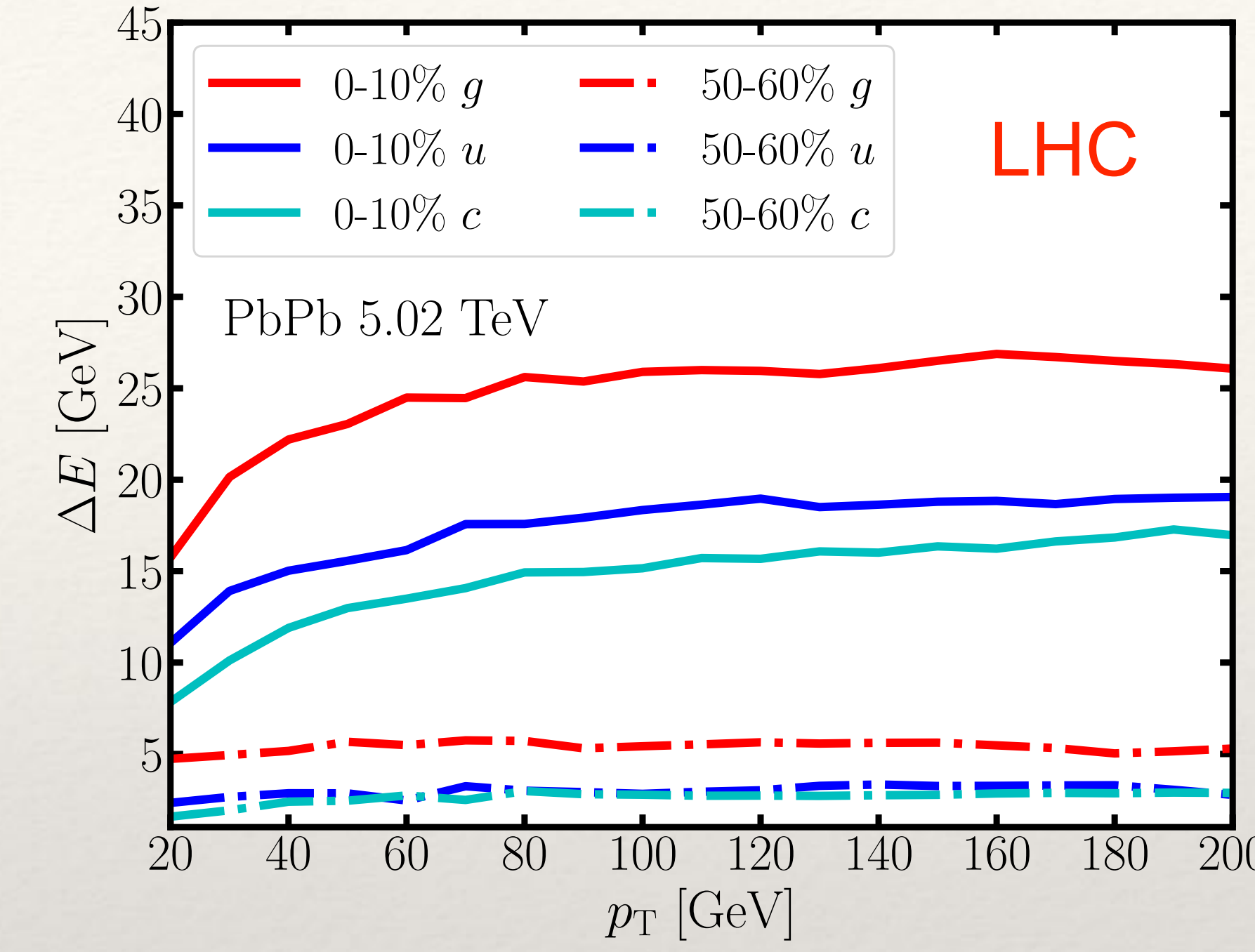
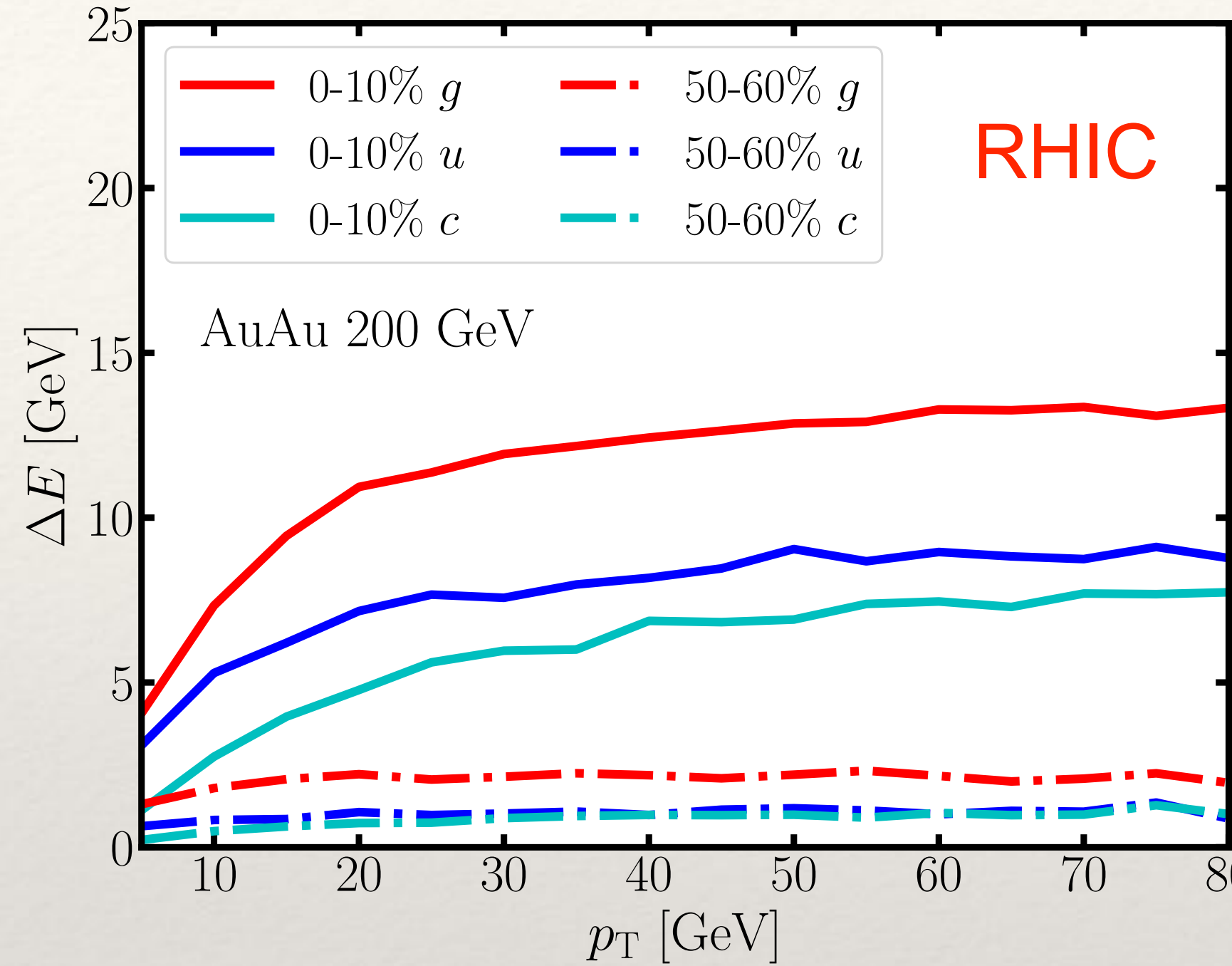
$$\frac{d\sigma_{\lambda_1 \lambda_2}^{\text{AA}}}{d\eta_1 d^2 \vec{p}_{\text{T}1} d\eta_2 d^2 \vec{p}_{\text{T}2}} = \int dx dy T_{\text{A}}(x - \tilde{b}/2, y) T_{\text{A}}(x + \tilde{b}/2, y) \int \frac{dz_1}{z_1^2} \frac{dz_2}{z_2^2} \sum_{ab \rightarrow cd} \sum_{\lambda_c \lambda_d} \frac{1}{\pi} x_a f_{\text{A},a}(x_a) x_b f_{\text{A},b}(x_b)$$

$$\times \frac{d\hat{\sigma}_{\lambda_c \lambda_d}^{ab \rightarrow cd}}{dt} \mathcal{D}_c(z_1, \lambda_1; \lambda_c) \mathcal{D}_d(z_2, \lambda_2; \lambda_d) \delta^2 \left(\frac{\vec{p}_{\text{T}1}}{z_1} + \Delta \vec{p}_{\text{T}1} + \frac{\vec{p}_{\text{T}2}}{z_2} + \Delta \vec{p}_{\text{T}2} \right) + \{c \leftrightarrow d\}.$$

- Nuclear modification:
 - Nuclear modified PDF (cold nuclear matter effect) — CTEQ PDF + EPPS shadowing
 - Parton energy loss in QGP: calculated using transport model (production location dependent)
 - Production location — nuclear thickness function from Woods-Saxon distribution
- In the end:

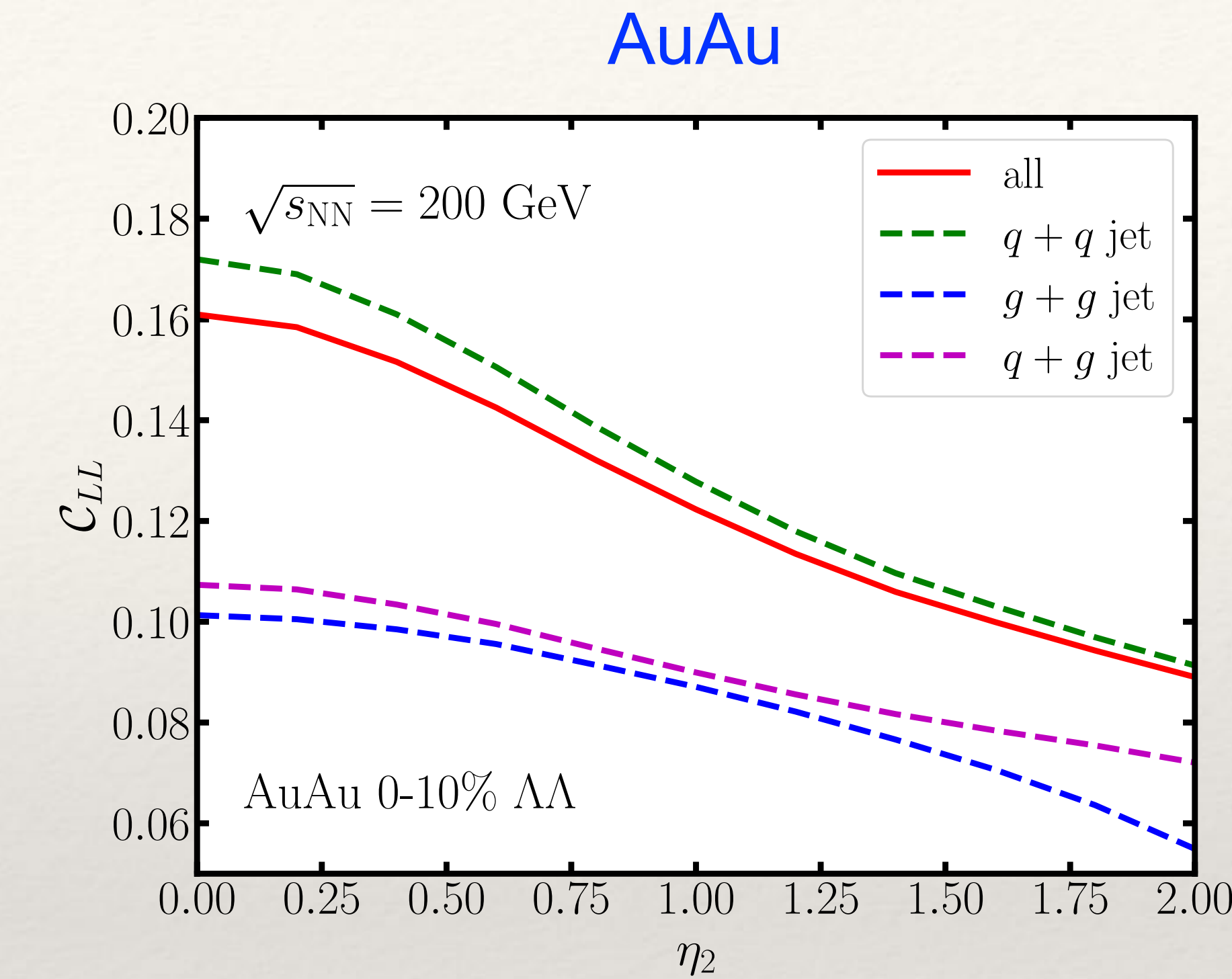
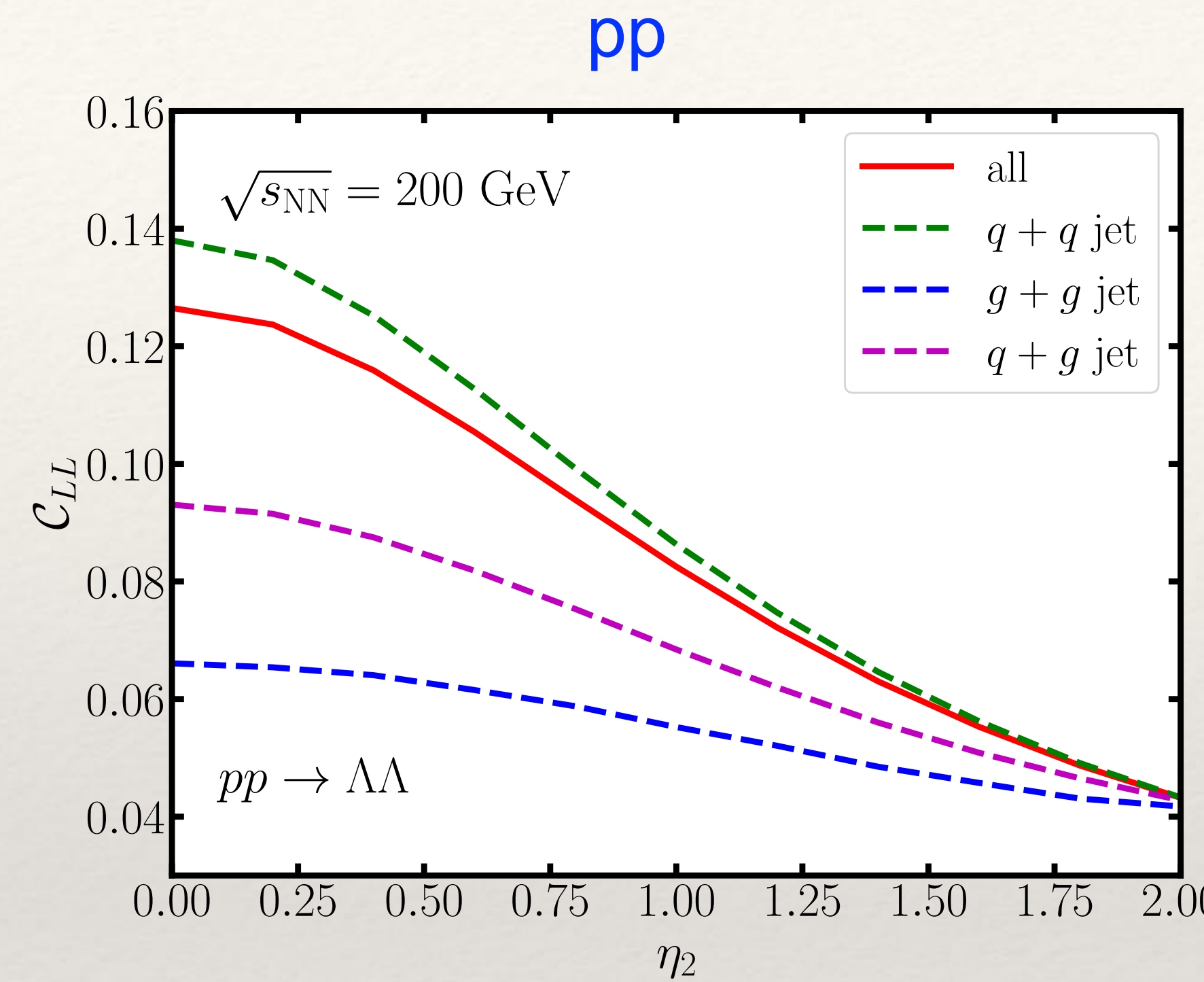
$$\mathcal{C}_{\text{LL}}(\eta_1, \eta_2) = \left(\frac{d\sigma_{\lambda_1=\lambda_2}}{d\eta_1 d\eta_2} - \frac{d\sigma_{\lambda_1=-\lambda_2}}{d\eta_1 d\eta_2} \right) \Bigg/ \left(\frac{d\sigma_{\lambda_1=\lambda_2}}{d\eta_1 d\eta_2} + \frac{d\sigma_{\lambda_1=-\lambda_2}}{d\eta_1 d\eta_2} \right)$$

Energy loss of different flavors of partons



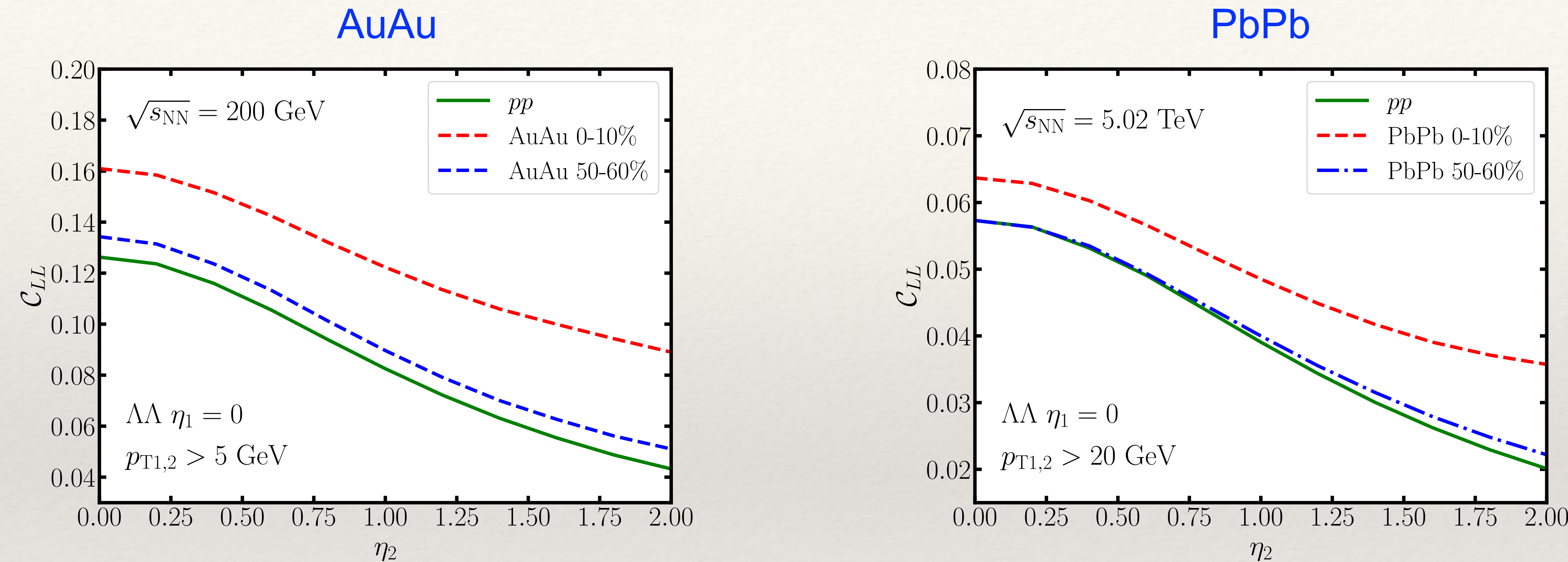
- Calculated using linear Boltzmann transport (LBT) model + hydrodynamic model
[SC, T. Luo, G.-Y. Qin, X.-N. Wang, Phys. Rev. C 94 (2016) 1, 014909]
- Flavor hierarchy of parton energy loss: $\Delta E_g > \Delta E_{u/d/s} > \Delta E_c$
- Stronger energy loss is more central collisions, and in more energetic collisions

Correlation of dihadron polarization in pp vs. AA



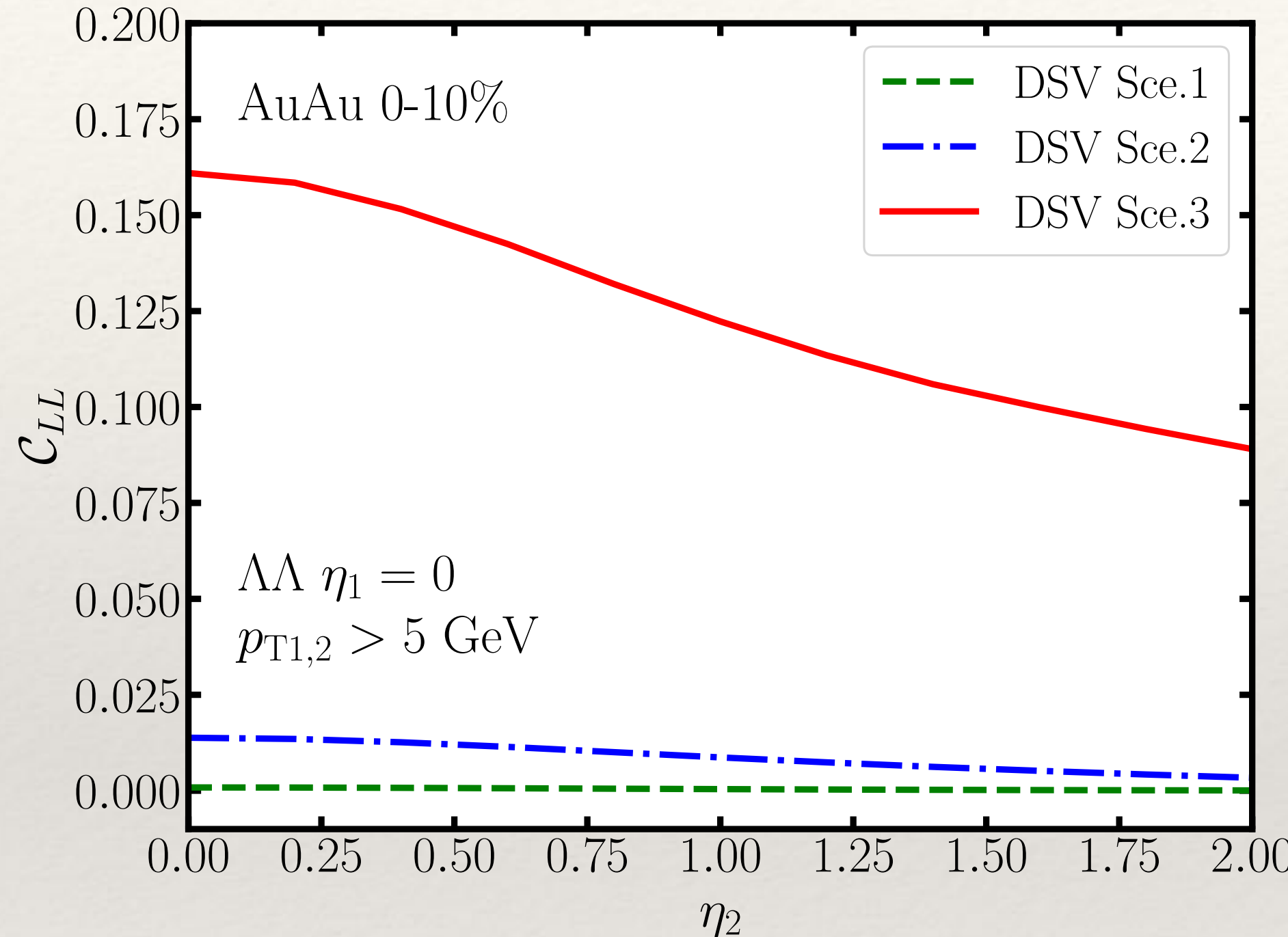
- Stronger spin correlation in AuAu than in pp — parton energy loss, hadron with the same final p_T probes larger z region of FFs
- Stronger enhancement for gluons than for quarks
- At the same final p_T , energy loss increases quark vs. gluon fraction \rightarrow enhance the total \mathcal{C}_{LL}

From pp to peripheral to central AA collisions



- Increase of \mathcal{C}_{LL} from pp to peripheral to central AA collisions

Constraint on the spin-dependent FFs

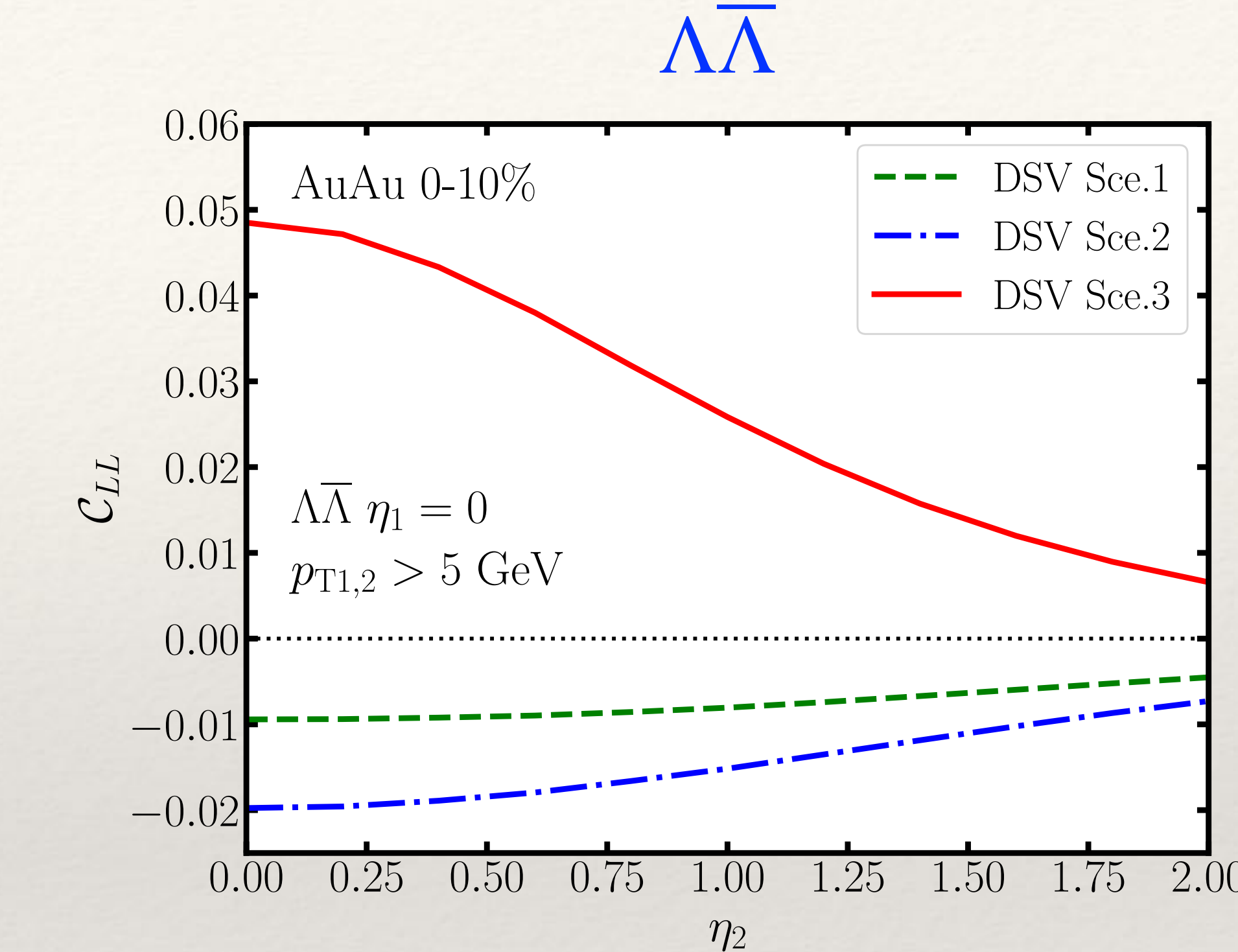
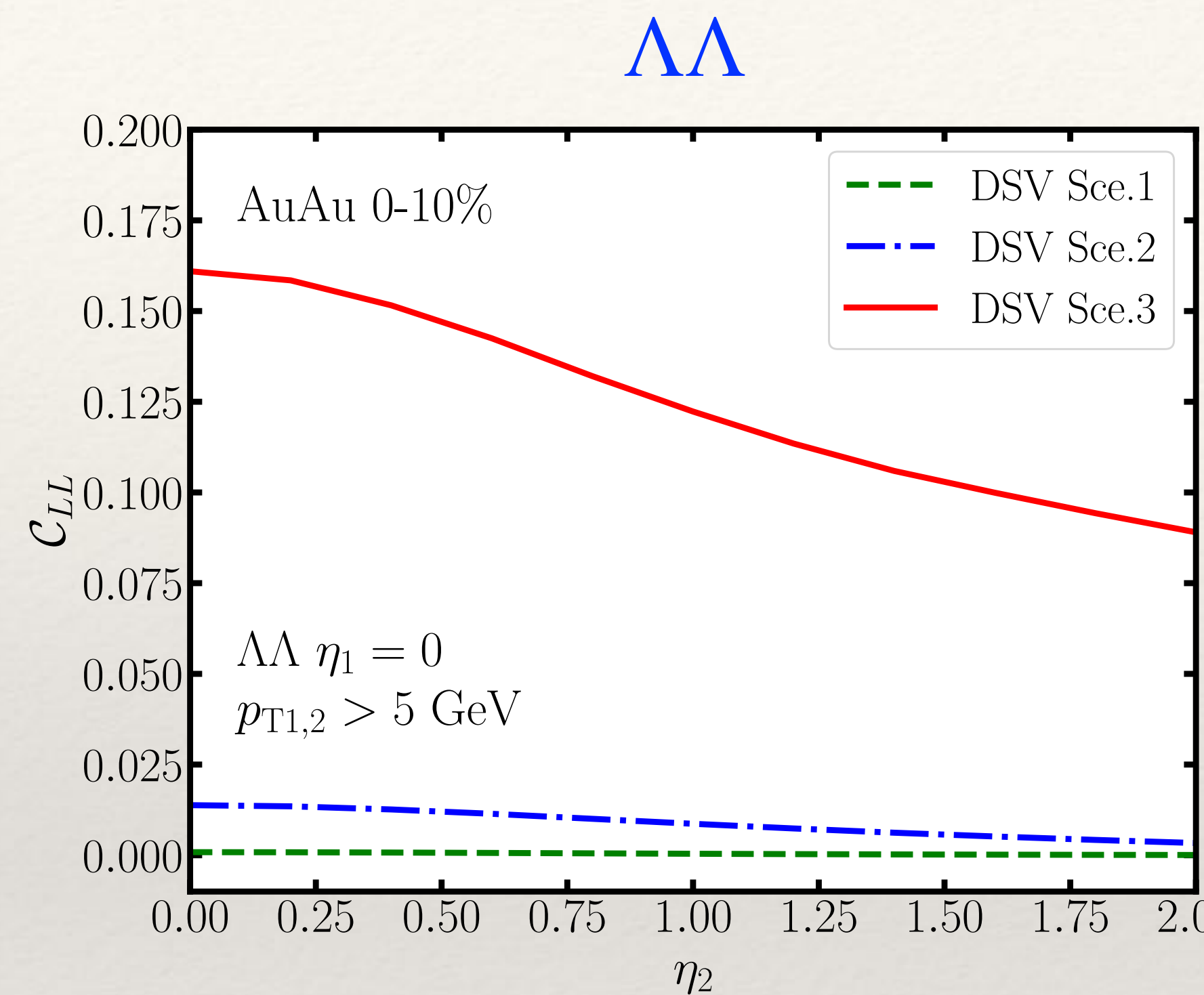


Comparison between 3 scenarios of DSV FFs (all tuned to spin-independent data)

- Scenario 1: only s transfers longitudinal spin to Λ
- Scenario 2: s has positive contribution, u and d have small negative contributions
- Scenario 3: u, d, s contribute equally to the polarized parts of FFs

C_{LL} can be used to constrain the longitudinal spin transfer in FFs

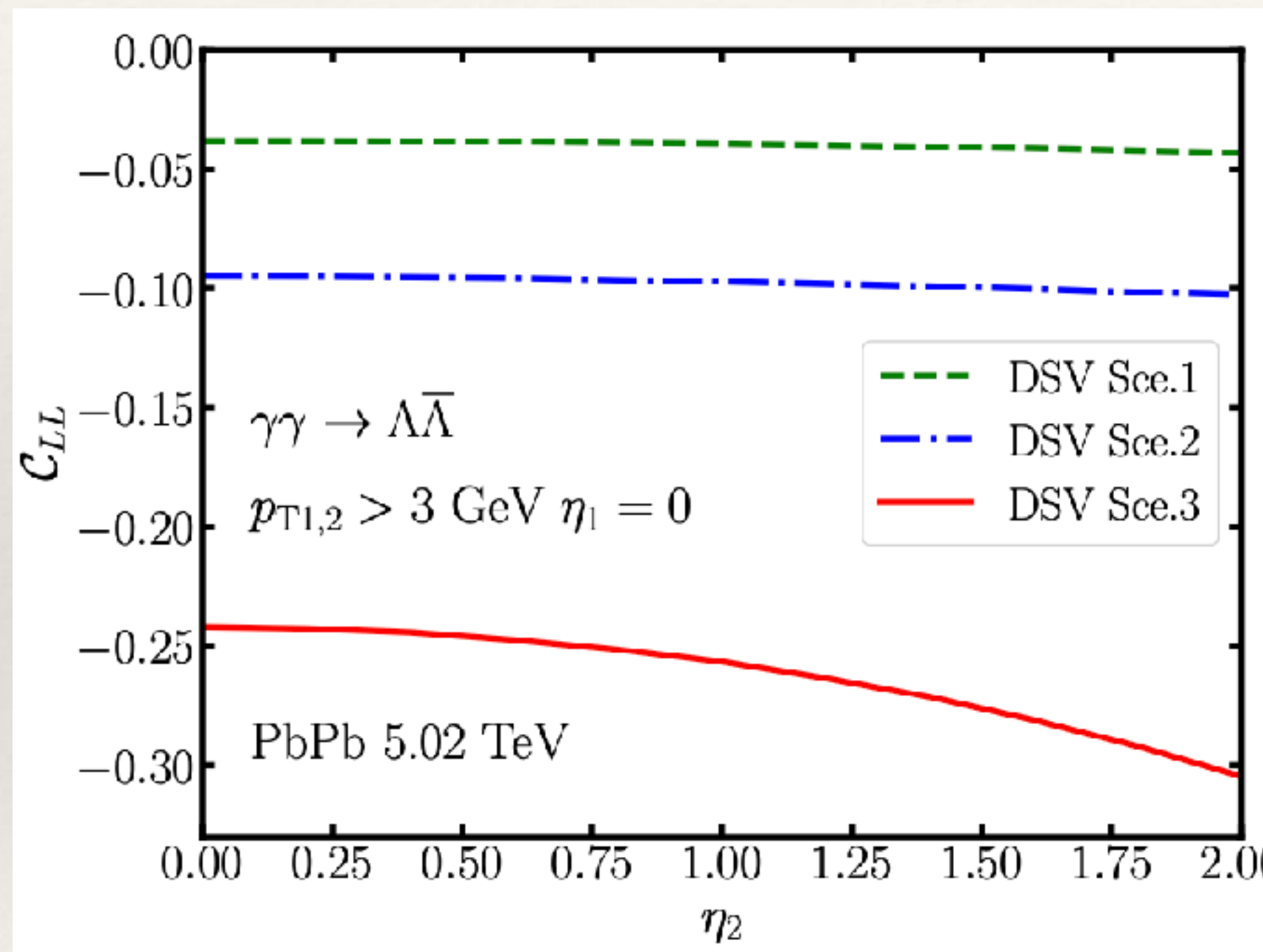
Comparison between $\Lambda\Lambda$ and $\Lambda\bar{\Lambda}$ correlations



- Scenario 1 reflects contributions from s-channel $s\bar{s}$ production, negative \mathcal{C}_{LL}
- \mathcal{C}_{LL} of $\Lambda\bar{\Lambda}$ is also sensitive to the selection of spin-dependent FFs

$\Lambda\bar{\Lambda}$ correlation in ultraperipheral collisions

- $\gamma\gamma \rightarrow \Lambda\bar{\Lambda}$ process



$$\frac{d\sigma^{\gamma\gamma}}{d\eta_1 d\eta_2} = \int dz_1 dz_2 \int \frac{d^2 \vec{p}_{T1}}{z_1^2} x_1 f_\gamma(x_1) x_2 f_\gamma(x_2) \sum_q \frac{1}{\pi} \frac{d\hat{\sigma}^{\gamma\gamma \rightarrow q\bar{q}}}{dt}$$

$$\times \left[D_{1,q}^\Lambda(z_1) D_{1,\bar{q}}^{\bar{\Lambda}}(z_2) - \lambda_1 \lambda_2 G_{1L,q}^\Lambda(z_1) G_{1L,\bar{q}}^{\bar{\Lambda}}(z_2) \right].$$

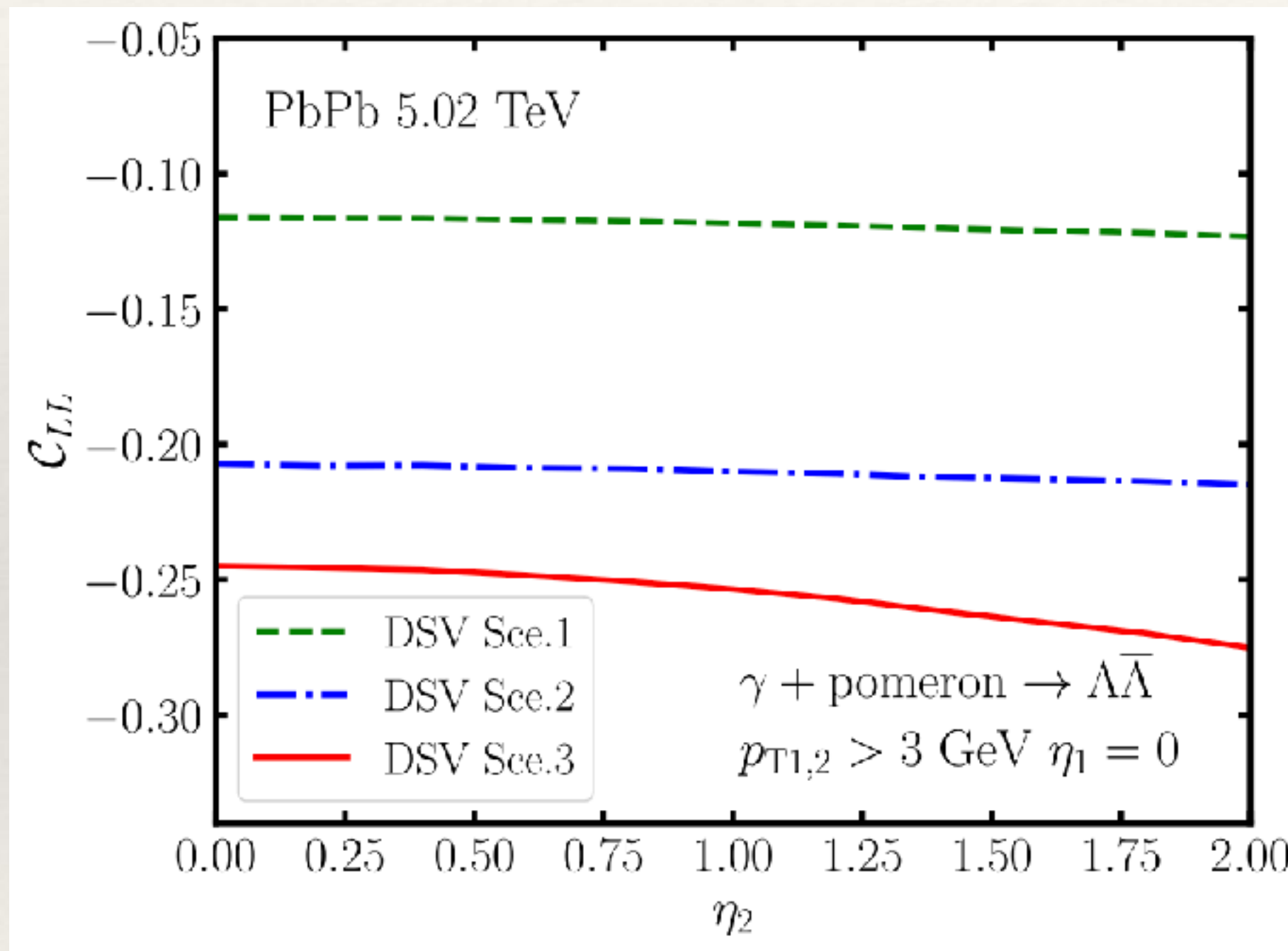
Hard cross section:

$$\frac{d\hat{\sigma}^{\gamma\gamma \rightarrow q\bar{q}}}{dt} = \frac{6\pi\alpha^2 e_q^4 t^2 + u^2}{s^2 tu}$$

- Different flavor dependence from $e^+e^- \rightarrow q\bar{q}$ process (e_q^2)
- Stronger contribution from u than s quarks
- Correlation from Scenario 3 is almost an order of magnitude larger than correlation from Scenario 1

$\Lambda\bar{\Lambda}$ correlation in ultraperipheral collisions

- $\gamma\mathbb{P} \rightarrow \Lambda\bar{\Lambda}$ process



$$\frac{d\sigma^{\gamma\mathbb{P}}}{d\eta_1 d\eta_2} = \int \frac{dx}{x} \int dz_1 dz_2 \int \frac{d^2 \vec{p}_{T1}}{z_1^2} x_1 f_\gamma(x_1) x g_{\mathbb{P}}(x, Q^2) \sum_q \frac{1}{\pi} \frac{d\hat{\sigma}^{\gamma\mathbb{P} \rightarrow q\bar{q}}}{dt}$$

$$\times \left[D_{1,q}^\Lambda(z_1) D_{1,\bar{q}}^{\bar{\Lambda}}(z_2) - \lambda_1 \lambda_2 G_{1L,q}^\Lambda(z_1) G_{1L,\bar{q}}^{\bar{\Lambda}}(z_2) \right].$$

Hard cross section:

$$\frac{d\hat{\sigma}^{\gamma\mathbb{P} \rightarrow q\bar{q}}}{dt} = \frac{\pi \alpha \alpha_s e_q^2}{s^2} t^2 + u^2$$

- Same flavor dependence as $e^+e^- \rightarrow q\bar{q}$ process
- Less difference between different scenarios of FFs compared to the previous $\gamma\gamma \rightarrow \Lambda\bar{\Lambda}$ process
- Supplementary channel to e^+e^- for studying polarized FFs

Summary

- Developed a perturbative approach for both initial production and spacetime evolution of quark polarization in relativistic heavy-ion collisions
- Found sensitivity of global polarization to the initial geometry of the QGP
- Studied the correlation of dihadron polarization (\mathcal{C}_{LL}) from jet fragmentation
- Found enhancement of \mathcal{C}_{LL} from pp to peripheral AA and then to central AA collisions due to the increasing parton energy loss inside the QGP, and sensitivity of \mathcal{C}_{LL} to the longitudinal spin transfer in polarized FFs

Spatial distribution of quark polarization

Spin-independent probability for a quark from nucleus A

$$\mathcal{P}_A(x_A, y_A) = \int T_2(x_B, y_B) \frac{d\sigma(x_A, y_A, x_B, y_B)}{dx_B dy_B} dx_B dy_B$$

Spin-dependent probability for a quark from nucleus A

$$\Delta\mathcal{P}_A(x_A, y_A) = \int T_2(x_B, y_B) \frac{d\Delta\sigma(x_A, y_A, x_B, y_B)}{dx_B dy_B} dx_B dy_B$$

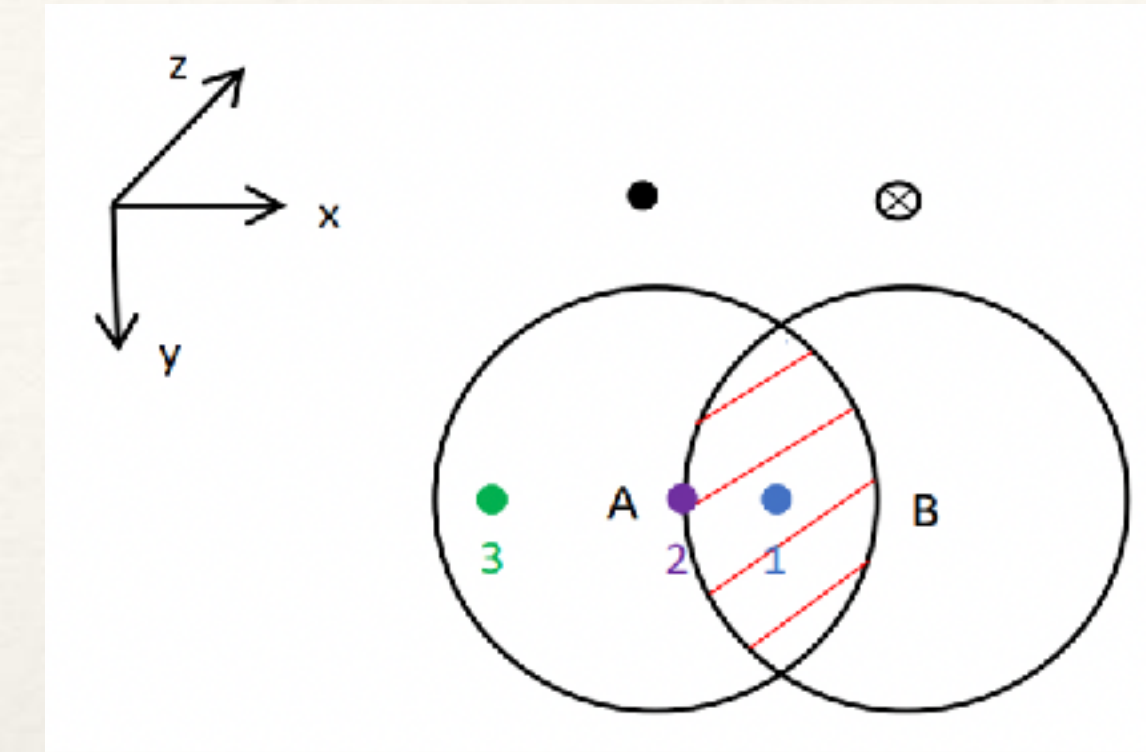
Spatial distribution of quark polarization

$$P(x, y) = \frac{T_1(x, y)\Delta\mathcal{P}_A(x, y) + T_2(x, y)\Delta\mathcal{P}_B(x, y)}{T_1(x, y)\mathcal{P}_A(x, y) + T_2(x, y)\mathcal{P}_B(x, y)}$$

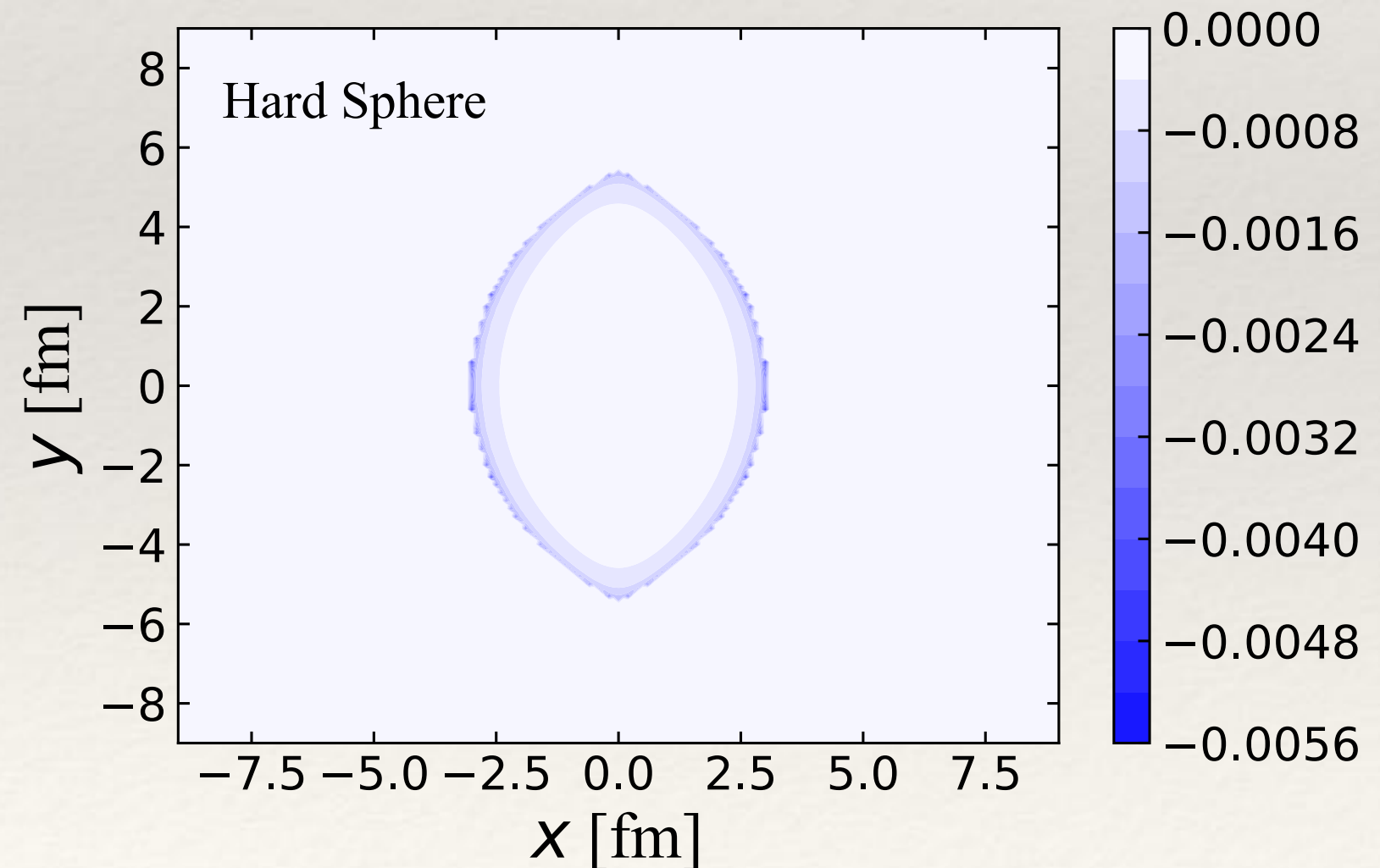
Spatial distribution of polarization from initial hard collisions

$$P(x, y) = \frac{T_1(x, y)\Delta\mathcal{P}_A(x, y) + T_2(x, y)\Delta\mathcal{P}_B(x, y)}{T_1(x, y)\mathcal{P}_A(x, y) + T_2(x, y)\mathcal{P}_B(x, y)}$$

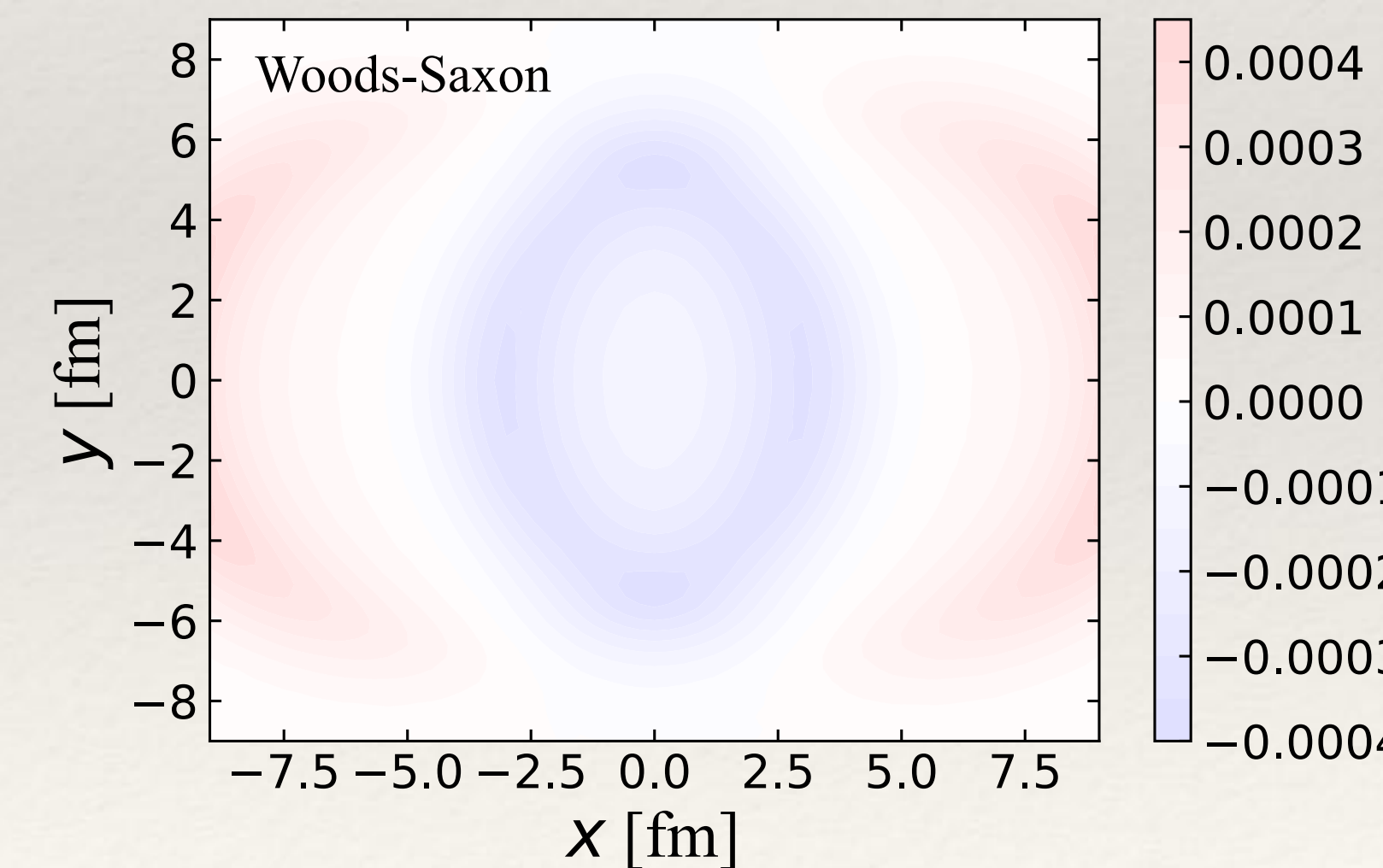
For 5-40% Au+Au @ 200 GeV



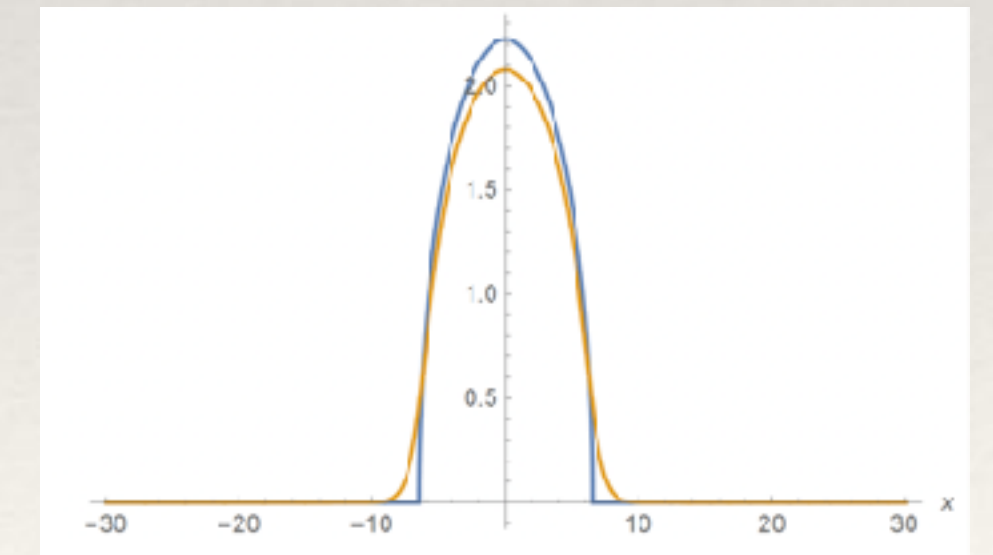
From Hard Sphere distribution



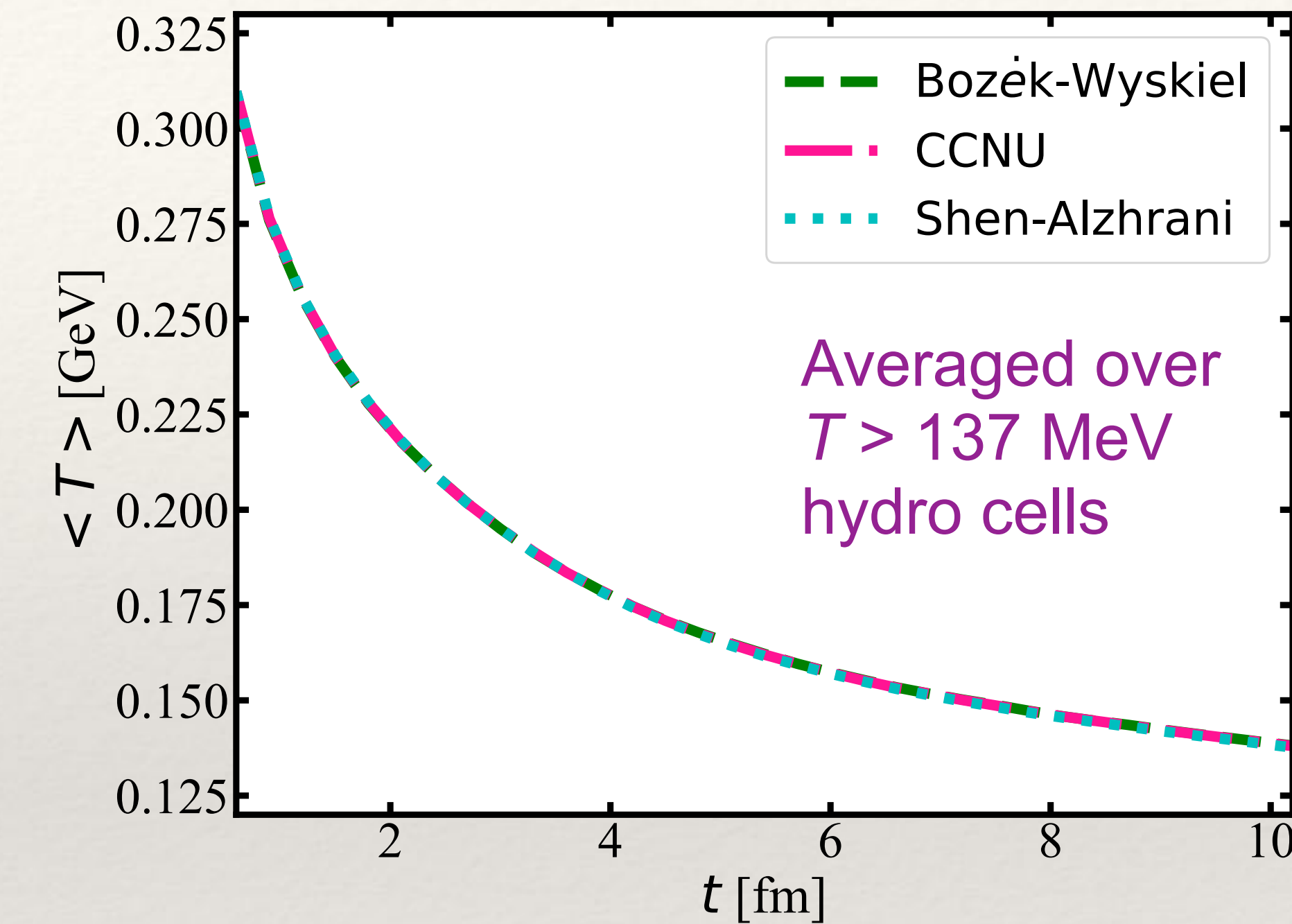
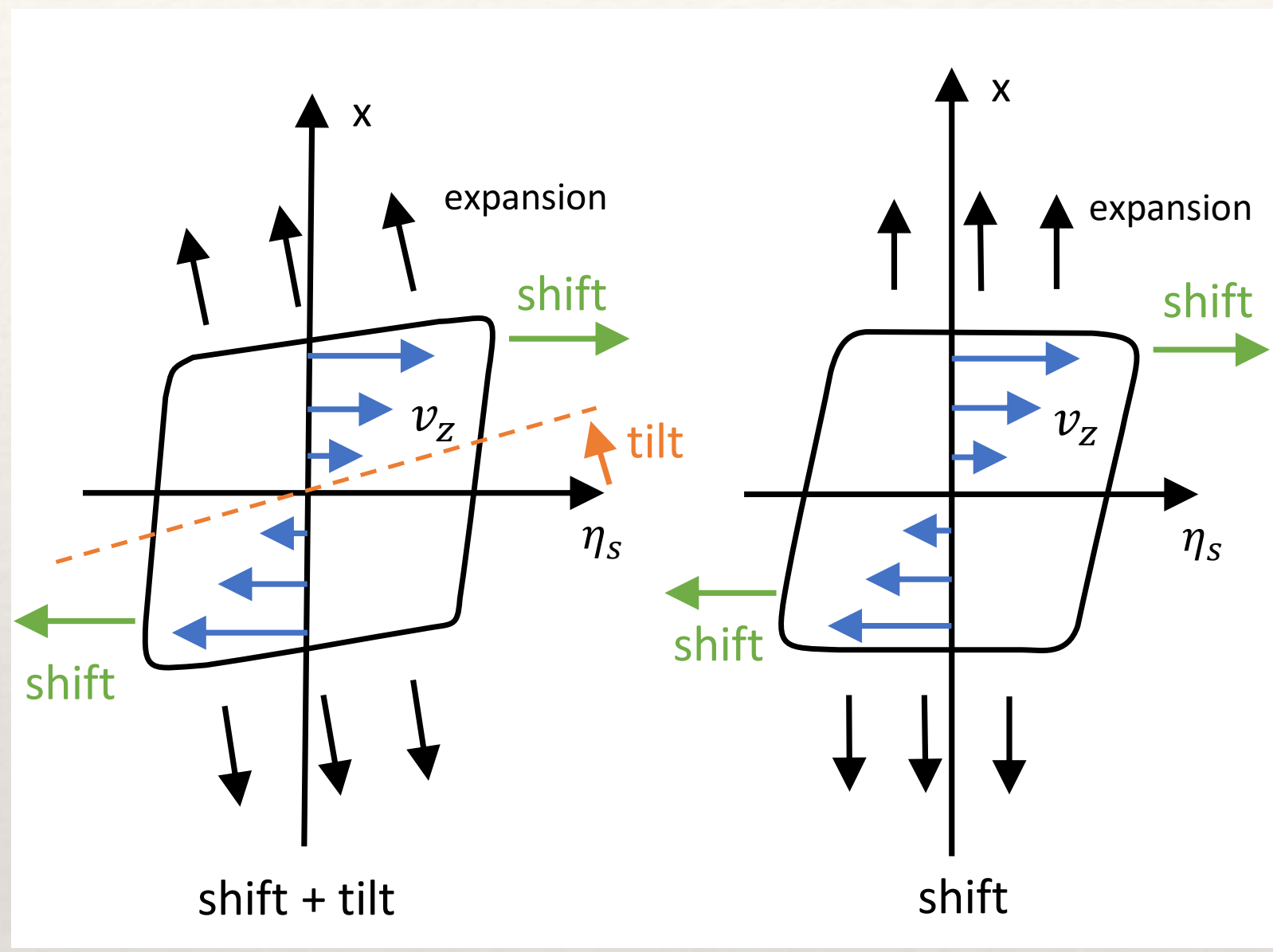
From Woods-Saxon distribution



Hard Sphere (HS)
Woods-Saxon (WS)

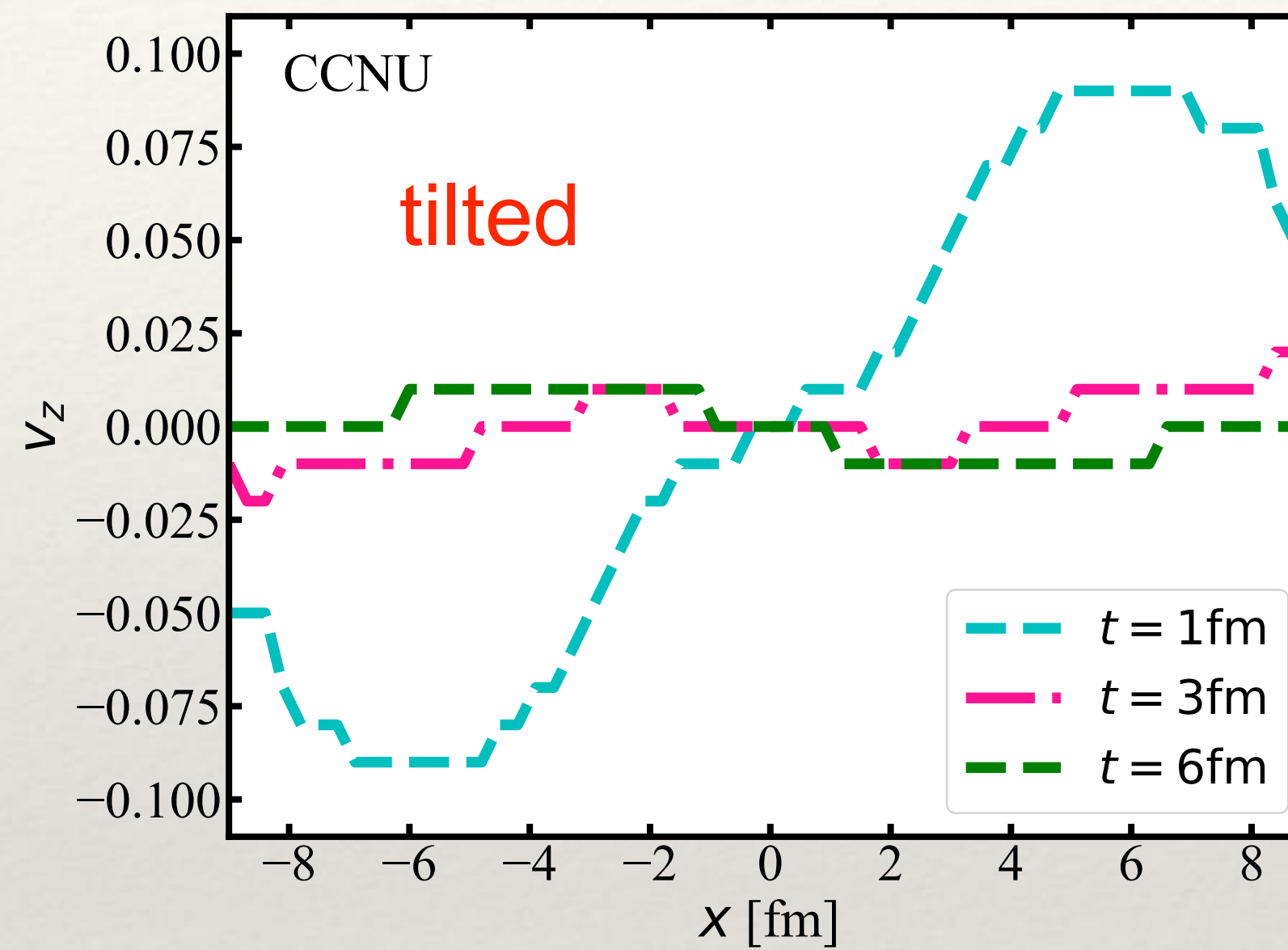


Evolution of average temperature

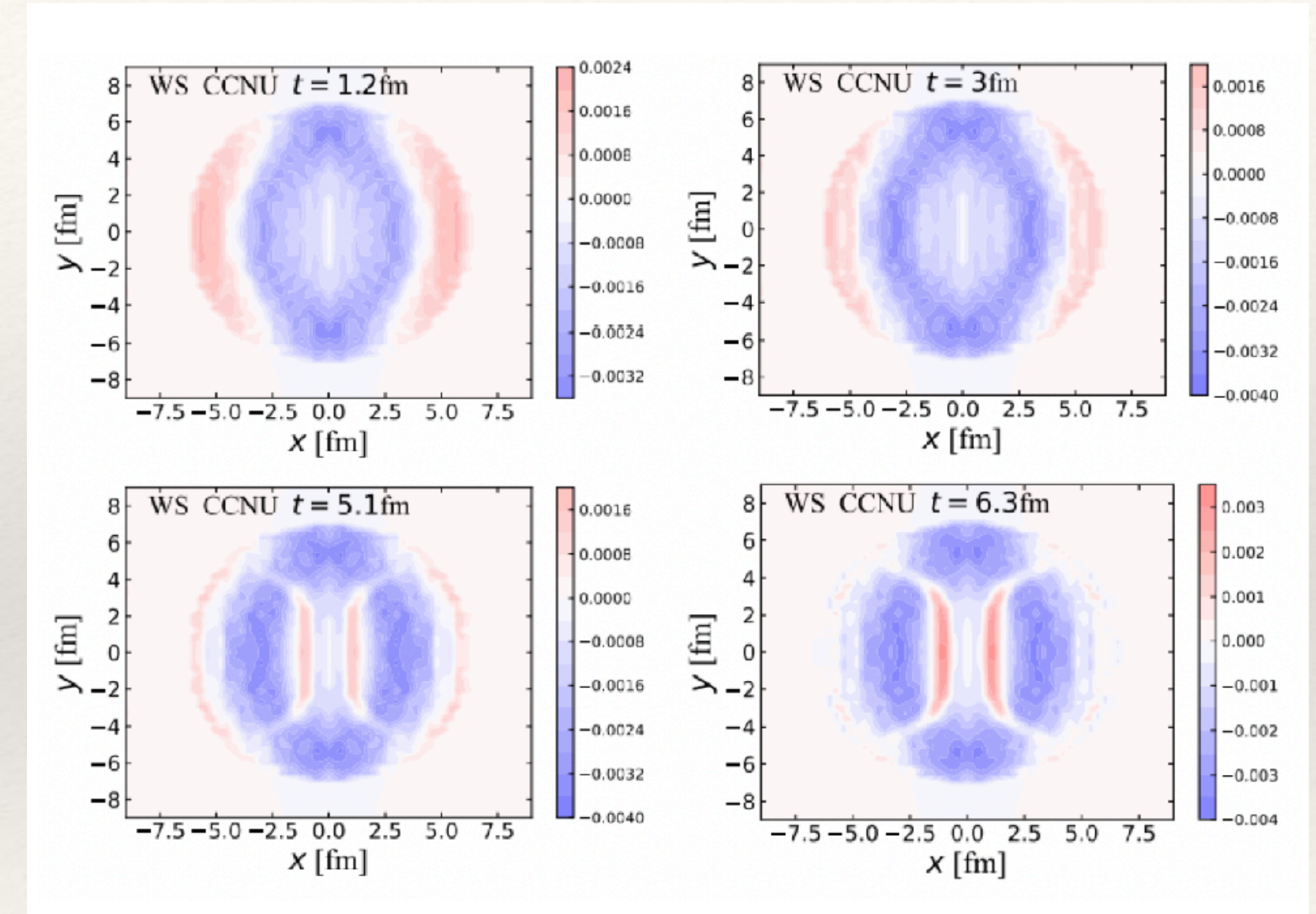


Consistent temperature evolution profiles between the three initial condition models

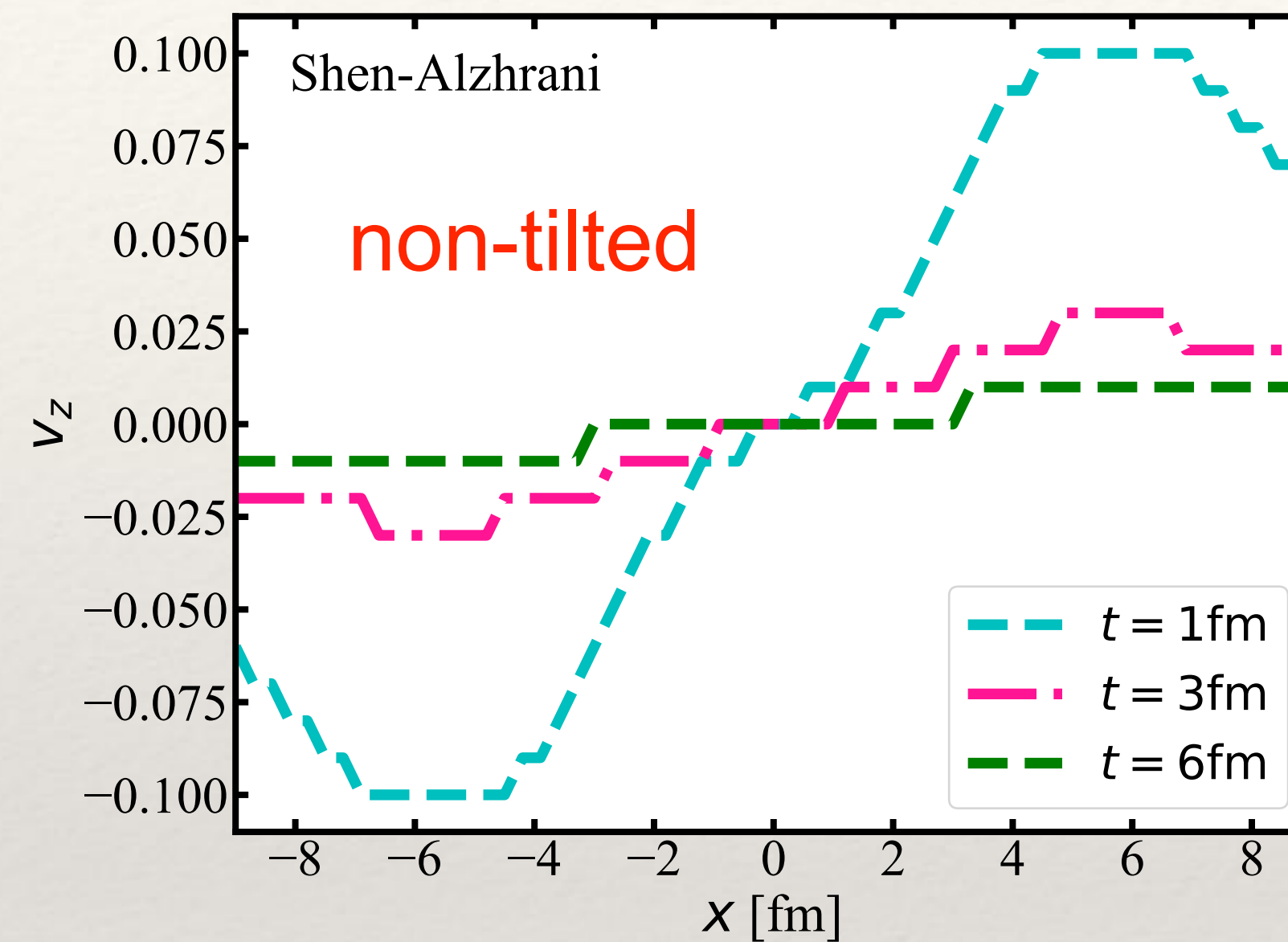
Spatial distribution of polarization with tilted initial geometry



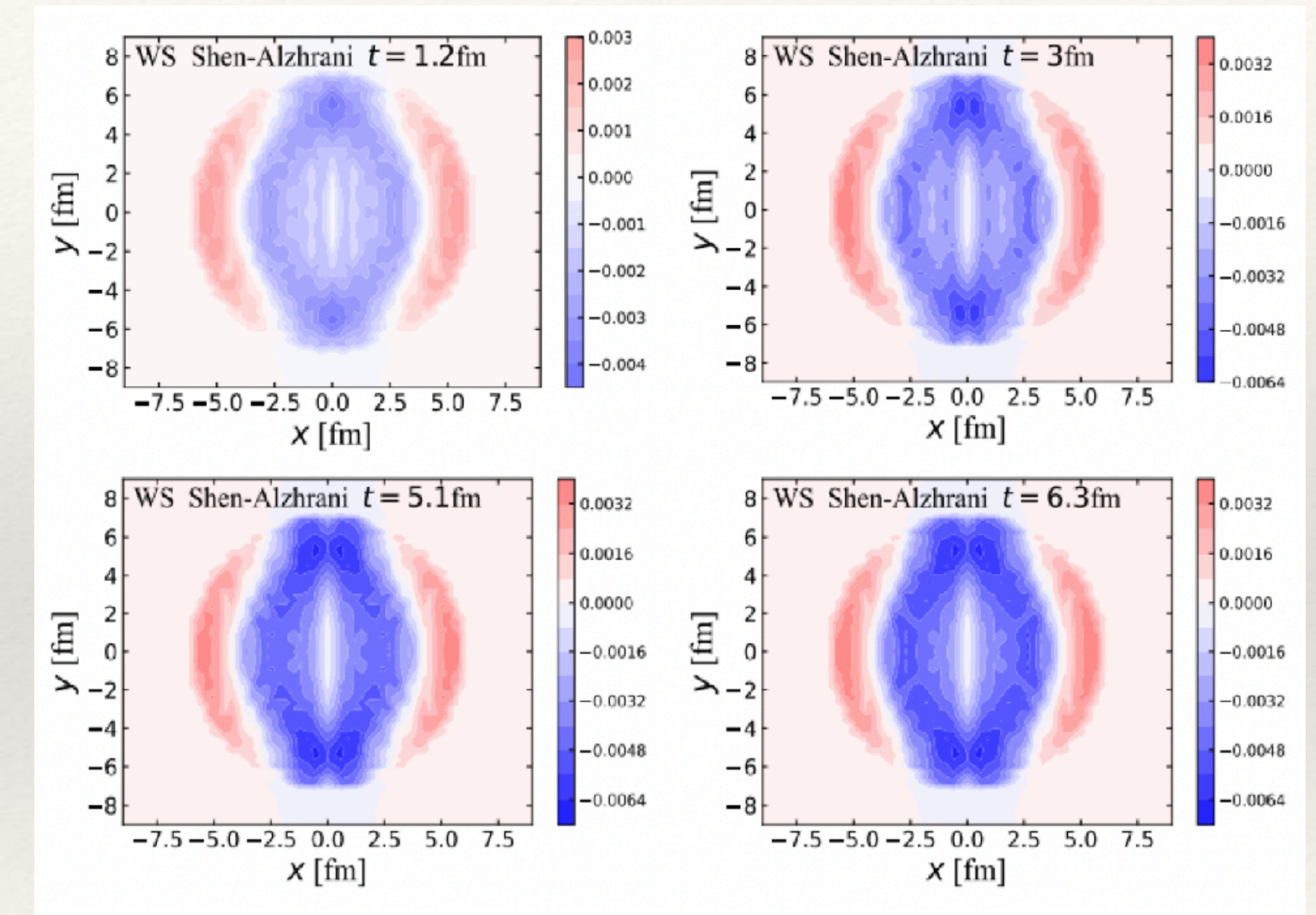
- The velocity gradient is the main origin of polarization generated inside the QGP



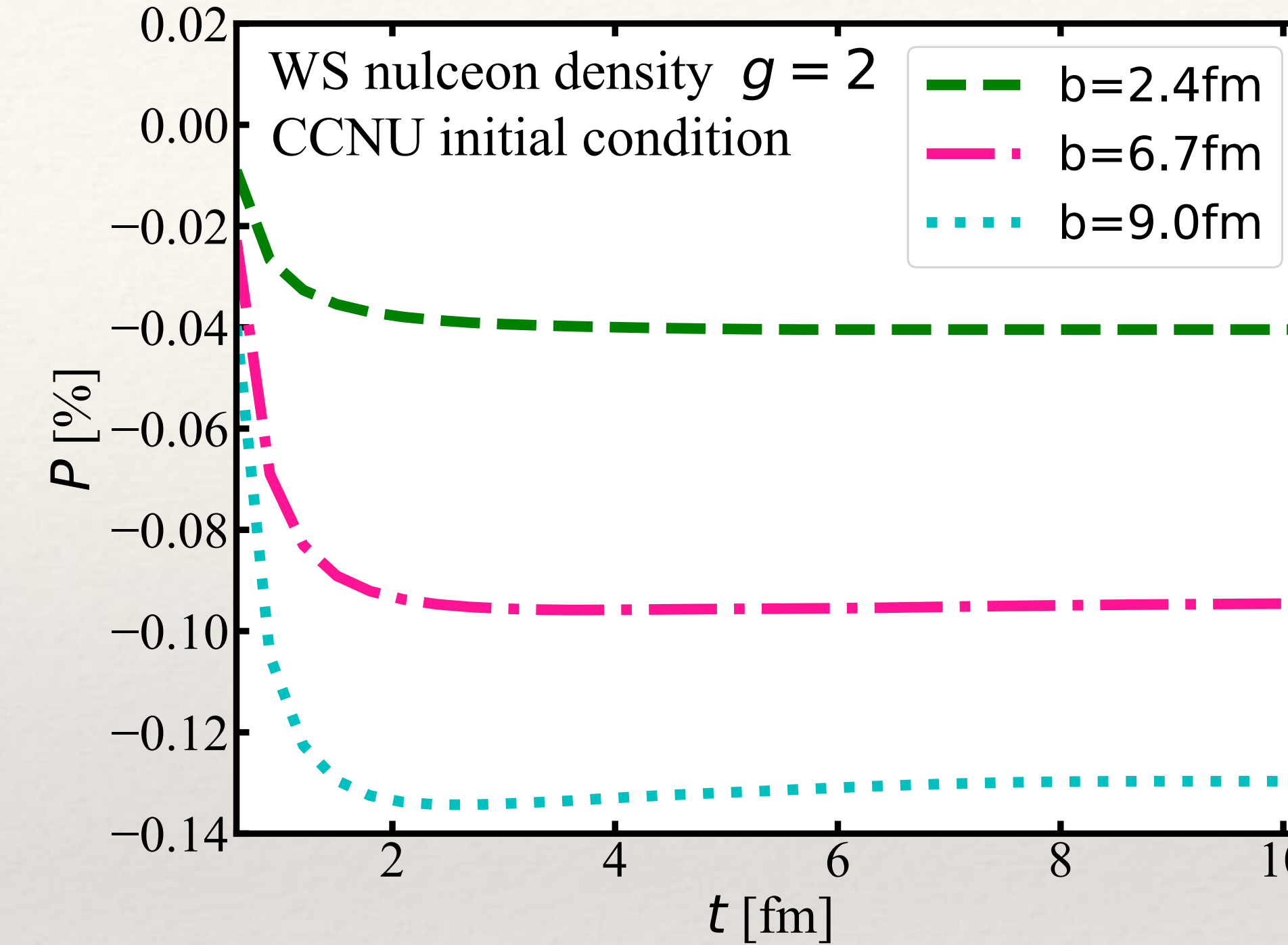
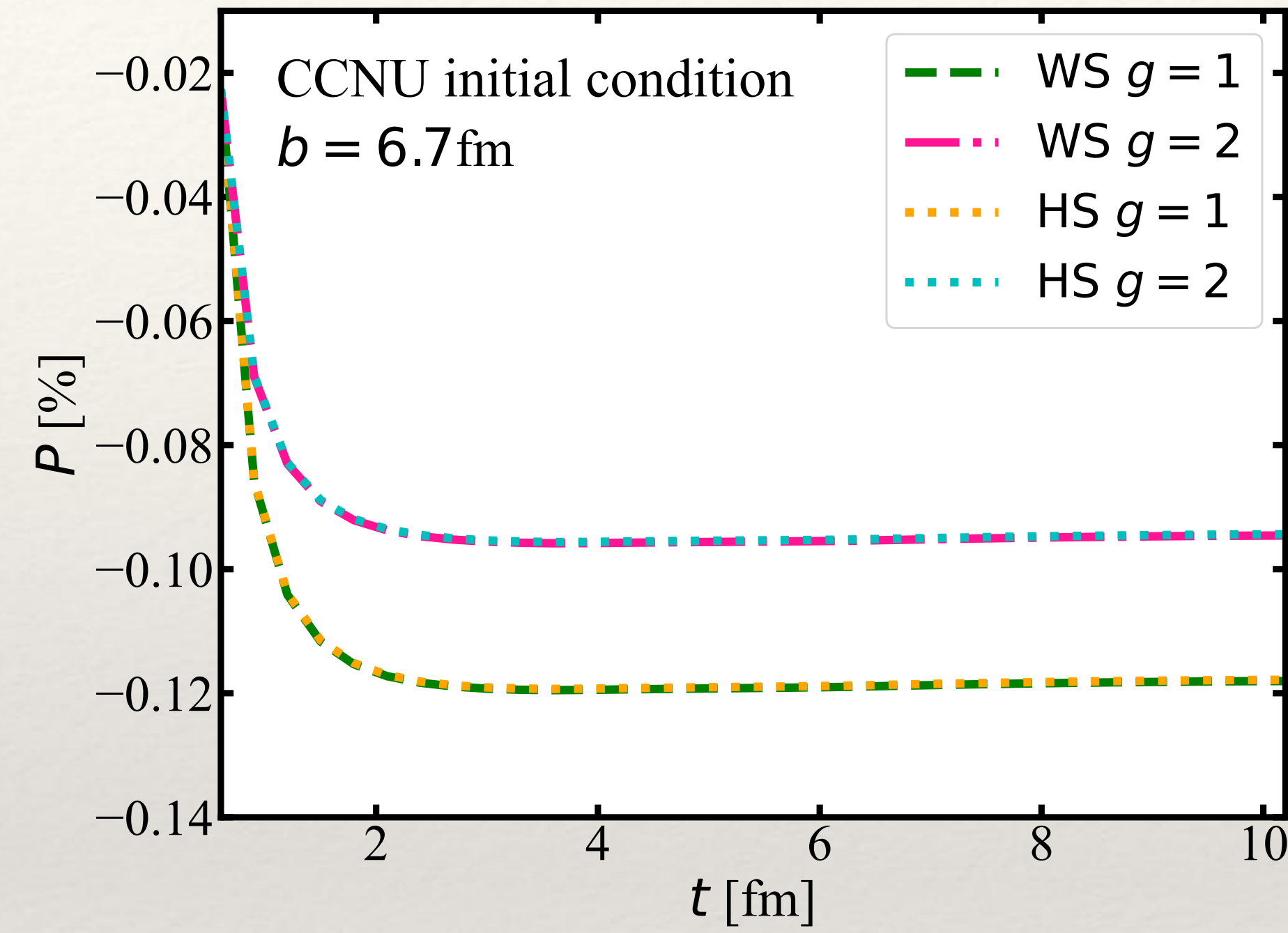
Spatial distribution of polarization with non-tilted geometry



- No sign flip for polarization with non-tilted initial geometry of QGP

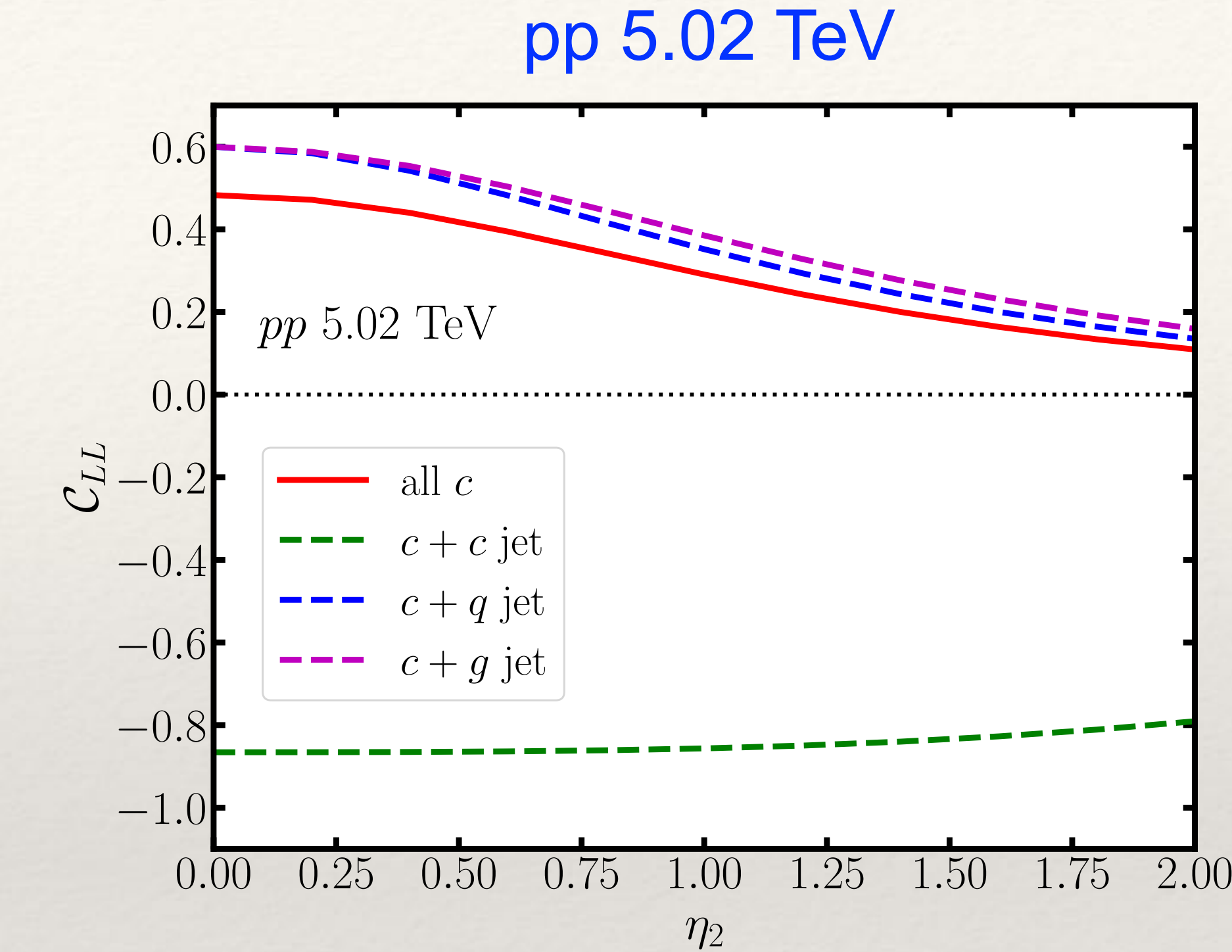
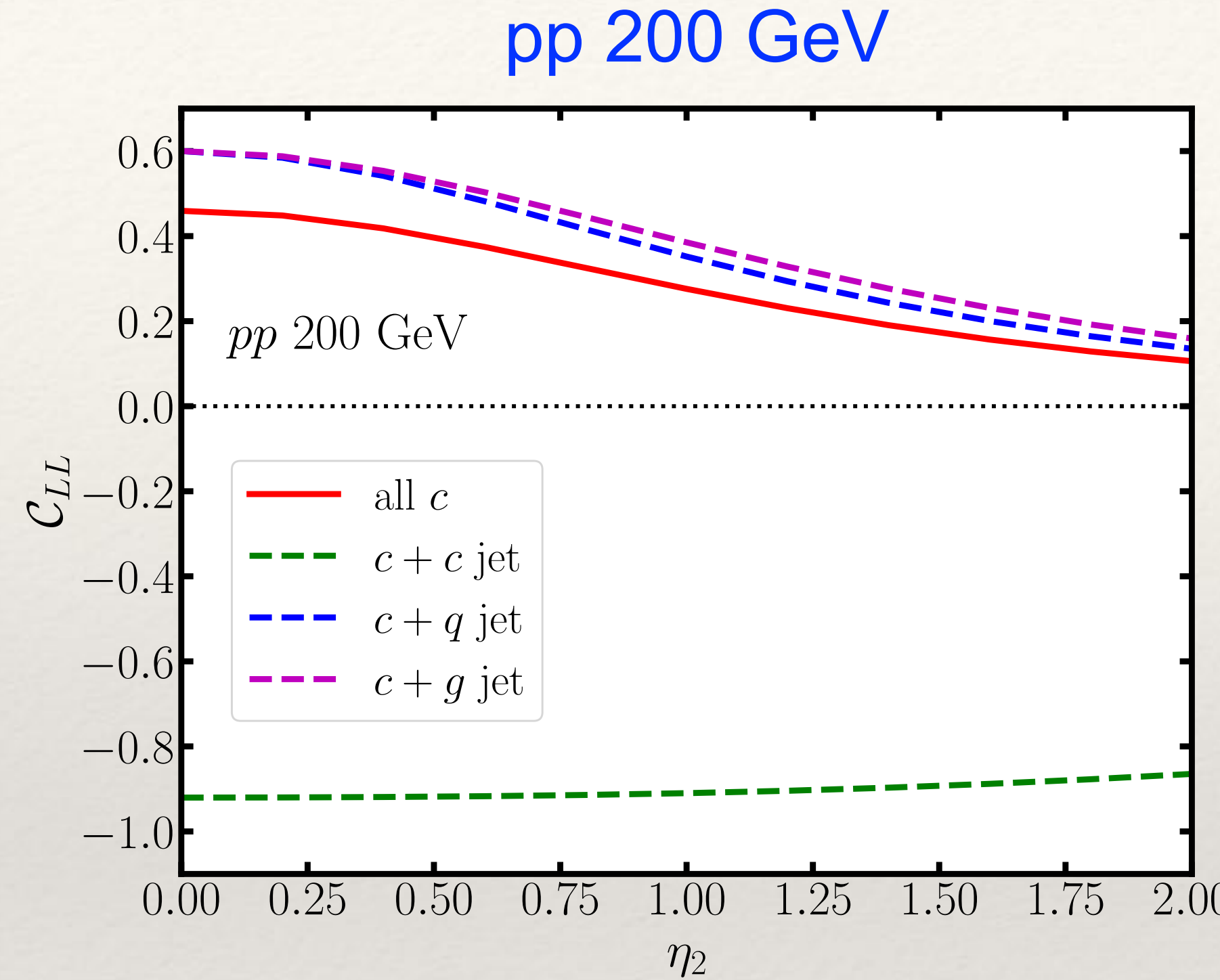


Time evolution of the average global polarization



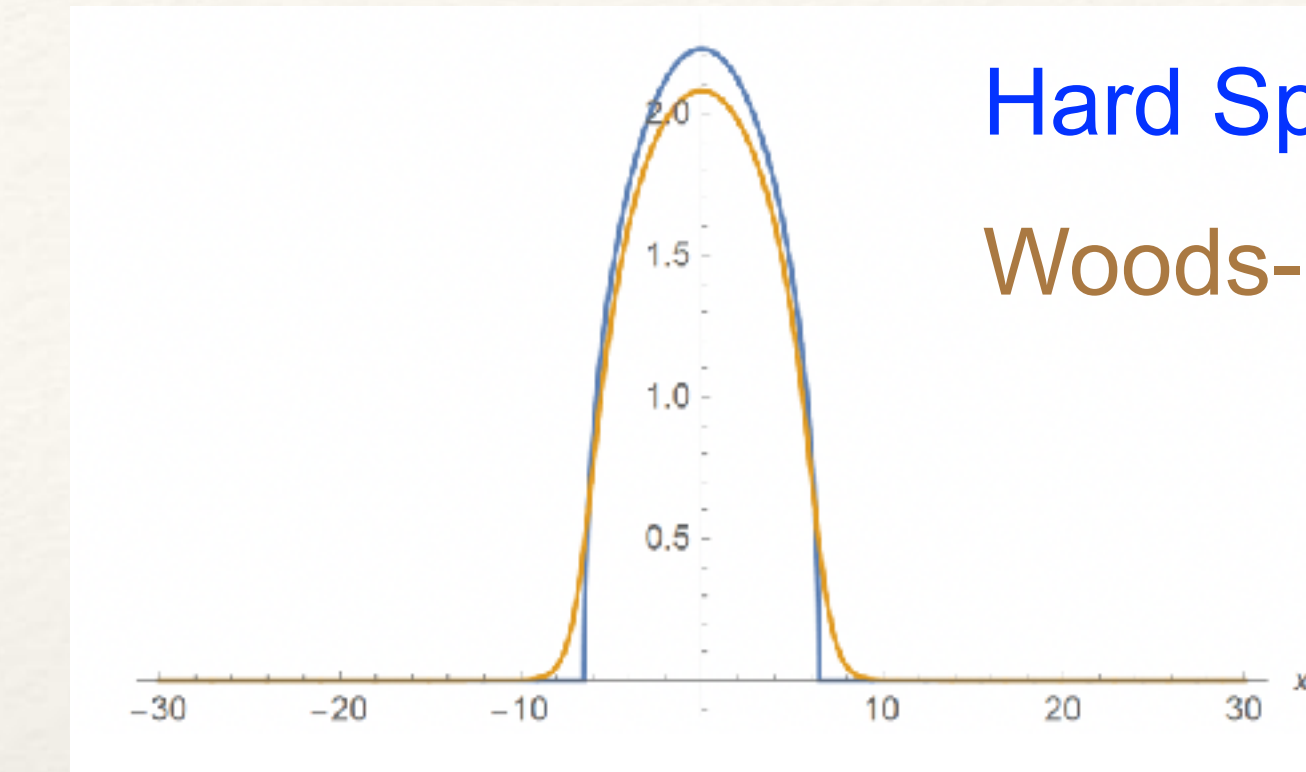
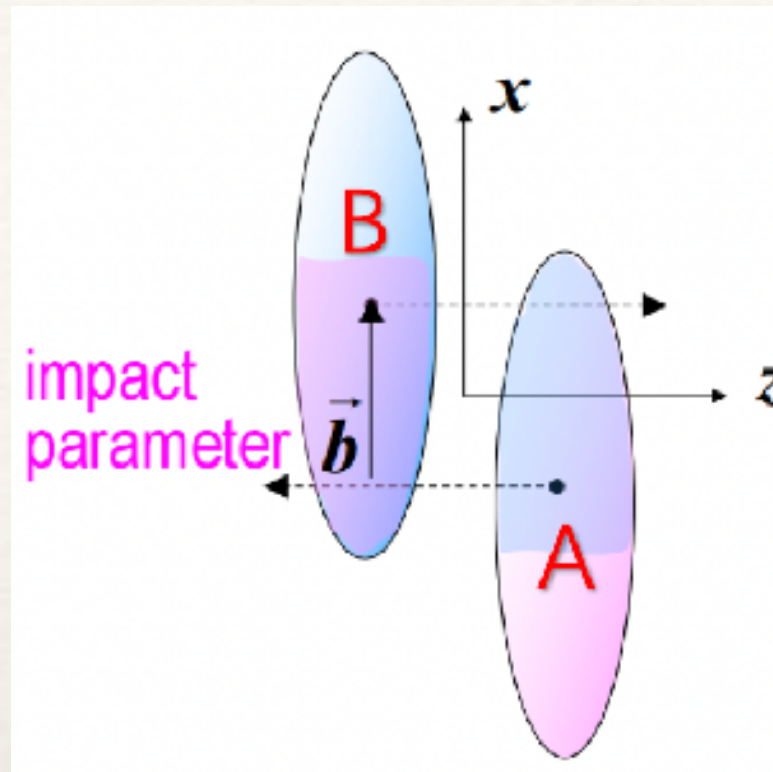
- Negligible dependence on the nuclear density distribution for the average polarization
- Decrease of polarization with increase of the coupling strength (via μ_D)
- Significant increase of polarization with impact parameter

Correlation between charm quark and another parton



- Results at partonic level (lack of spin-dependent FFs for c)
- Different charm production mechanism (pair production, flavor excitation, gluon splitting)
- Strong negative C_{LL} of back-to-back $c\bar{c}$ may help constrain FFs to Λ_c in the future

Comparison between two distributions



Distribution in one nuclei

Hard Sphere:

$$T_{A,B}^{\text{HS}}(x, y) = \frac{3A}{2\pi R^3} \sqrt{R^2 - (x \pm b/2)^2 - y^2} \Theta(R - \sqrt{(x \pm b/2)^2 + y^2})$$

Woods-Saxon:

$$T_{A,B}^{\text{WS}}(x, y) = C_0 \int (1 + \exp \frac{\sqrt{(x \pm b/2)^2 + y^2 + z^2} - R}{a})^{-1} dz$$

Distribution of participants from one nuclei

Hard Sphere:

$$T_{1,2}^{\text{HS}}(x, y) = T_{A,B}^{\text{HS}} \Theta(R - \sqrt{(x \mp b/2)^2 + y^2})$$

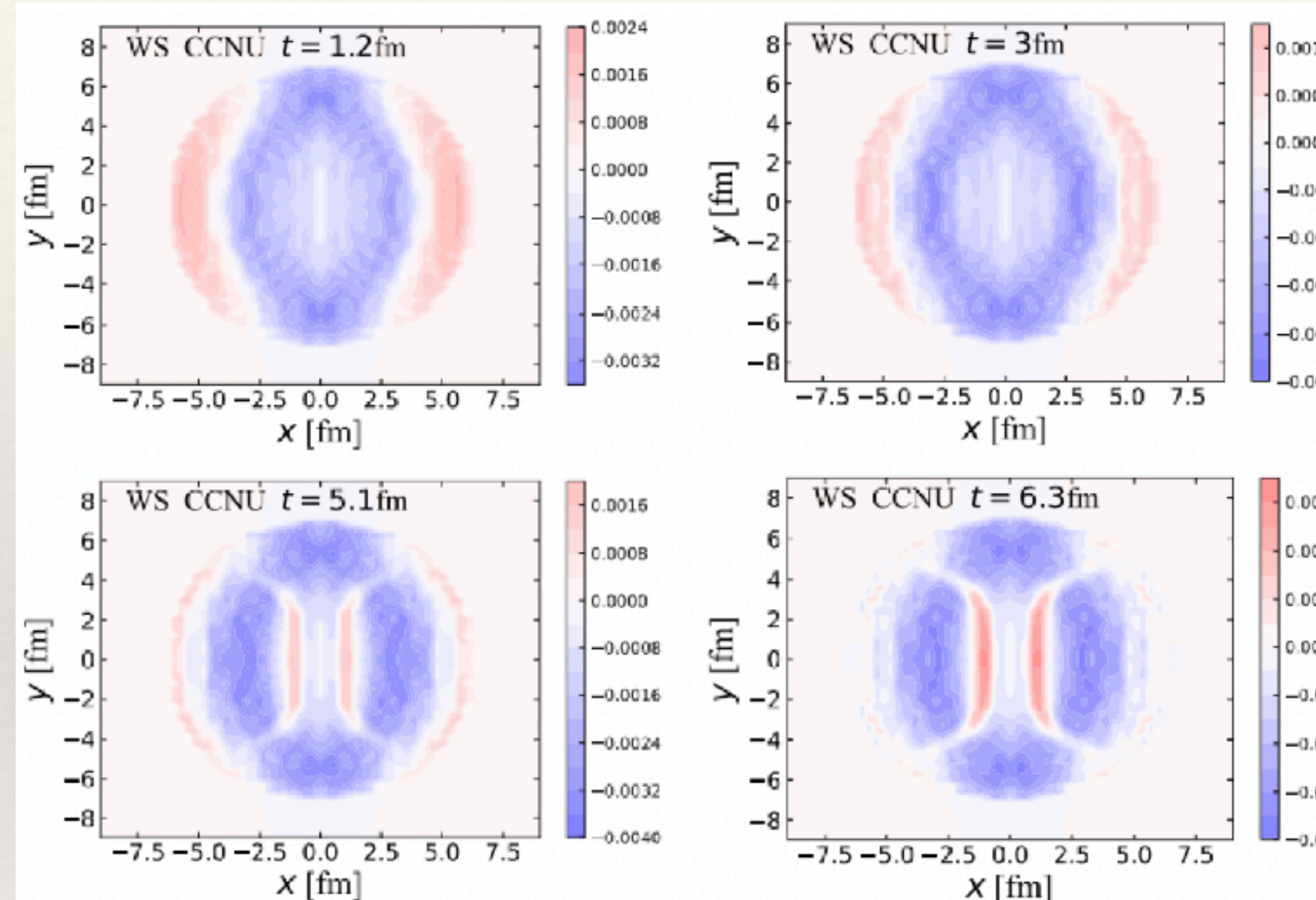
Woods-Saxon:

$$T_{1,2}^{\text{WS}}(x, y) = T_{A,B}^{\text{WS}} [1 - \exp(-\sigma_{\text{NN}} \times T_{B,A}^{\text{WS}})]$$

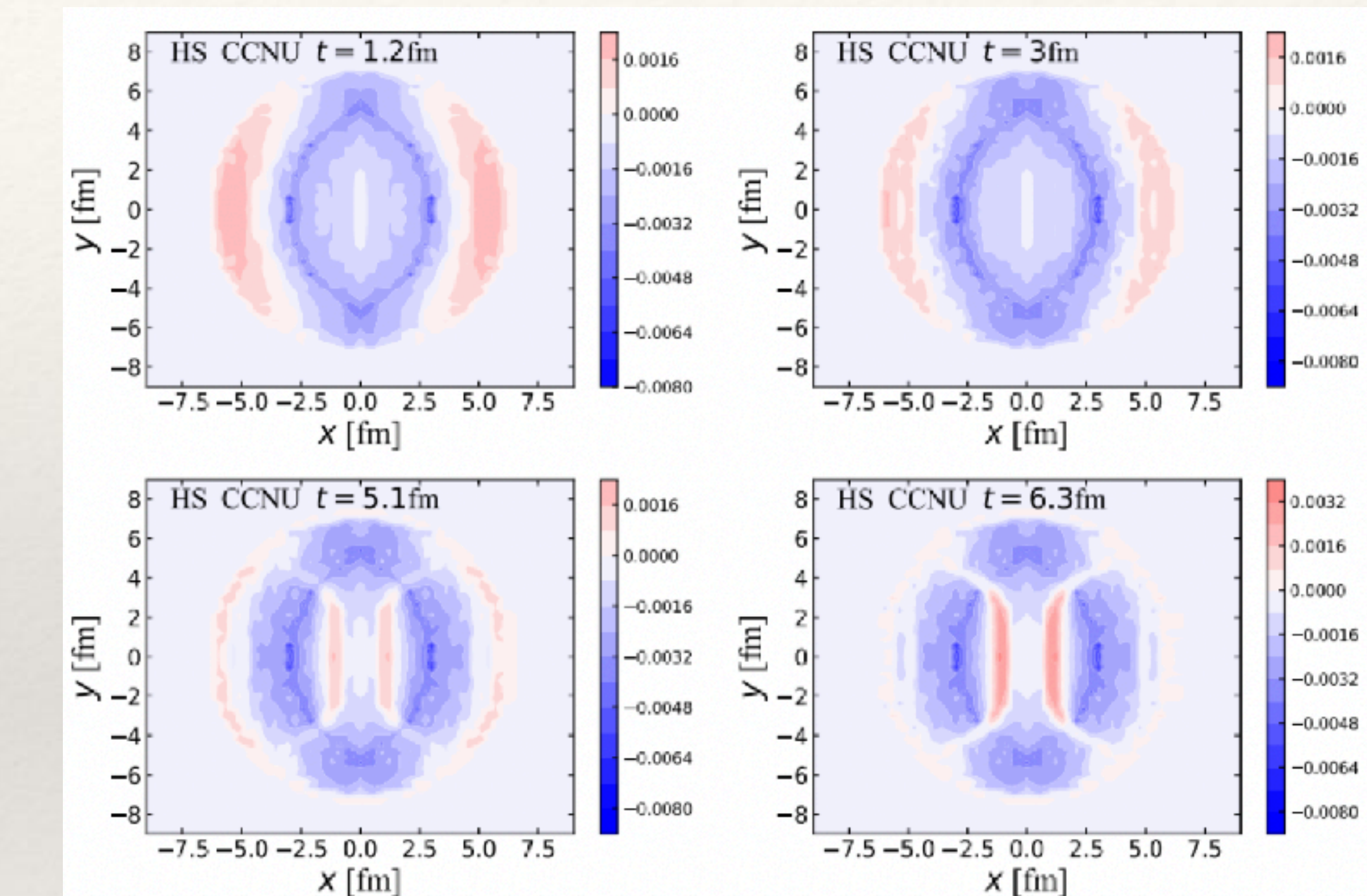
$$P = \frac{\int T(x, y) \frac{d\Delta\sigma(x, y)}{d^2 x_T} d^2 x_T}{\int T(x, y) \frac{d\sigma(x, y)}{d^2 x_T} d^2 x_T}$$

Effects of nuclear density distribution on polarization

Woods-Saxon



Hard Sphere



- Smoother distribution of quark polarization across the transverse plane from Woods-Saxon than from the Hard Sphere density distribution

